

1 system scale studies of distributive fluvial systems, to guide interpretations. Mapping showed these
2 formations to be highly heterogeneous with channel body proportion (from 12 to 81%) and geometry
3 types (large amalgamated bodies to isolated channels), grain size (silt to conglomerate), average channel
4 body thickness (4 to 20 m) and average storey thickness (3 to 10 m) varying significantly across the
5 basin. Distributive fluvial systems in the form of alluvial and fluvial fans in transverse configurations
6 were recognised as well as a wide axial system, with heterogeneity in the formations being closely
7 aligned to these interpretations. Furthermore, numerous individual depositional systems were identified
8 within the formations (Beartooth Absaroka, Washakie, Owl Creek and axial). Predicted downstream
9 distributive fluvial system trends (i.e. downstream decrease in channel proportion, size and grain size)
10 were identified in the Beartooth, Absaroka and Owl Creek systems. However, predicted trends were not
11 identified in the Washakie system where intrabasinal thrusting disturbed the sequence. Importantly, a
12 wide axial fluvial system was identified, where reverse downstream distributive fluvial system trends
13 were present, interpreted to be the result of the input of transverse systems of variable size. This study
14 provides a new level of detail in the application of basin-scale models, demonstrating their usefulness in
15 trying to understand and predict alluvial architecture distribution and heterogeneity, with important
16 implications for economic resources and palaeogeographic reconstructions.

17 **INTRODUCTION**

18 Sedimentary basins are areas in which tectonic subsidence of the Earth's crust has occurred, creating
19 accommodation within which sedimentary successions can be deposited and, importantly, be preserved
20 (e.g. Allen & Allen, 1990; Weissmann et al., 2010; Nyberg & Howell, 2015). By studying the deposits of
21 continental sedimentary basins, insights can be gained into past terrestrial environments, as well as
22 changes in climate, tectonics and base level, throughout Earth's history (Bridge, 2003). Due to the
23 different variations and combinations of these processes, resultant deposits can vary through time and
24 space, with a multitude of different deposit characteristics possible. The need for predictive models is

1 crucial in such instances because they enable common predictive facies and architectures to be
2 identified (Walker, 1984, 1990), as well as help better understand how changes in major processes can
3 affect the characteristics of deposits. Continental deposits also contain societally important resources,
4 housing ground water, petroleum reserves and mineral deposits. Therefore, for the successful
5 exploration and extraction of these resources, often conducted with spatially restricted datasets,
6 predictive models are key in reducing uncertainty in predictions as they aid current understanding and
7 increase the ability to predict potential variations in facies and sandstone body architectures within a
8 basin.

9 As noted by Walker (1984; 1990), in order to generate basin-scale predictive facies models, such as
10 those produced explicitly for extensional settings (e.g. Leeder & Gawthorpe, 1987 and Gawthorpe &
11 Leeder, 2000), integration of modern and ancient examples is required. However, at the basin scale few
12 studies try to bridge the gap between modern and ancient observations, with the two areas often not
13 working in conjunction with one-another (Davidson et al., 2011). Documented examples of modern
14 studies that assess geomorphic elements (i.e. fluvial fan, trunk/axial/tributary rivers and interfan areas)
15 within modern basins include the Pantanal Basin (Brazil)(e.g. Assine et al., 2015), the Okavango
16 (Botswana) (Stanistreet & McCarthy, 1993) and those discussed in Weissmann et al. (2015, e.g. the
17 Andean foreland basin, Horton & Decelles, 2001; the Himalayan foreland Basin, Sinha & Friend 1994; the
18 Rio Grande Rift, Mack & Seager, 1990). Studies of modern continental basins show distributive fluvial
19 systems (DFS) and axial fluvial systems to be common components of a basin fill (e.g. Mack & Seager,
20 1990; Sinha & Friend, 1994; Horton & Decelles, 2001; Assine et al., 2015; Weissmann et al., 2010, 2015).
21 Weissmann et al (2015), take this observation further by quantifying the extent of the four main
22 geomorphic elements identified in basins studied in their paper including DFS (including megafans,
23 fluvial fans, alluvial fans, bajada and incised DFS), tributive fluvial systems (axial and interfan), aeolian
24 and lacustrine depositional areas. The authors established that DFSs are the dominant geomorphic

1 element in the basins studied, with over 88% of the basin area covered by fluvial deposits on DFS, with
2 tributary systems (axial and interfan areas) composing only a small percentage (1 to 12%) of the
3 sedimentary basin surface area.

4 Although these studies offer valuable insights into basin filling processes, as is the issue with all studies
5 of modern depositional systems, these observations represent a snap-shot in time of the basin fill,
6 whereas rock-record studies allow an overview of the preserved basin-fill to be gained. Due to the
7 discontinuous nature of geological datasets, basin-scale rock-record fluvial studies often concentrate on
8 documenting the generalised stratigraphic architecture of basin fills or document the detailed
9 sedimentological characteristics at the outcrop and/or reservoir scale (e.g. Kukulski et al., 2013). As a
10 result there is a need for more studies that document the detail often done at the outcrop/reservoir
11 scale across entire depositional basins (Kukulski et al., 2013). Examples of studies on terrestrial deposits
12 at the basin scale include the Upper Cretaceous, Neuquén Basin of Argentina (Legarreta & Uliana, 1998),
13 the Upper Cretaceous Cordilleran Basin of south-west USA (DeCelles & Cavazza, 1999), Palaeocene Wind
14 River Basin (Seeland, 1978), the Cenozoic Gulf of Mexico (Galloway et al., 2011), Miocene to Pliocene
15 sediments in the Gediz Graben, Turkey (Çiftçi & Bozkurt, 2009), the Oligocene–Miocene deposits of the
16 northern portion of the Ebro Basin (Nichols & Hirst, 1998) and the Late Jurassic southern portion of the
17 Morrison Formation (Owen et al. 2015). However, many of these studies may be spatially restricted, or
18 focus on a particular type of dataset. In particular, few make parallels with modern basin scale studies or
19 test basin fill models.

20 This paper aims to document key sedimentological characteristics across an entire depositional basin to
21 test whether individual geomorphic elements can be identified (i.e. individual systems, rather than
22 taking mapping units as single entities), and aid interpretation of fluvial basin-fill successions. To achieve
23 this goal the Palaeocene Fort Union and Eocene Willwood formations across the Bighorn Basin,
24 Wyoming (USA) are analysed. In particular this study tests the applicability of the DFS model. Predictive

1 models for individual DFS are now relatively well-established from modern and rock-record based
2 studies, with a downstream decrease in channel amalgamation, proportion and size occurring
3 concurrently with increased floodplain preservation (e.g. Friend & Moody-Stuart, 1972; Kelly & Olsen,
4 1993; Weissmann et al., 2013) which has been quantitatively documented in only two studies (Hirst,
5 1991; Owen et al., 2015). However, the applicability of the model across an ancient sedimentary basin
6 has yet to be fully explored. It is hypothesised that the documented downstream trends of DFS should
7 be replicable across the basin, with the model essentially being 'up-scaled' across an entire basin, based
8 on observations made by Weissmann et al. (2013) in modern studies. To test this, downstream trends in
9 palaeocurrent, grain size, channel body thickness, proportion and grain size together with channel
10 geometry type distribution were analysed across the basin to assess how well they relate to predicted
11 trends for DFSs.

12 **METHODS**

13 To achieve these aims, architectural panels and sedimentary logs from 28 locations across the basin (12
14 from the Fort Union Formation, 16 from the Willwood Formation) (Fig. 1) were collected. A total of 4192
15 m of sedimentary logs was collected across 8700 km² of the basin. From these field-based data,
16 statistical information on key characteristics, such as palaeocurrent trends, grain size, channel body and
17 storey thickness, channel presence and geometry were obtained. These datasets were interrogated
18 individually, and were integrated to produce a palaeogeographic model for the Bighorn Basin in which
19 systems are deduced. Where possible, a mammalian age group was assigned (Palaeocene, undiff;
20 Tiffanian; Clarkforkian; Wasatchian-1 to 4; Wasatchian-5 to 7) based on the work of Gingerich & Clyde
21 (2001) allowing approximate correlations and construction of a biostratigraphically constrained
22 framework. Channel body geometries in the Bighorn Basin have been previously described and defined
23 by Owen et al., (2017b). Geometry types were defined based on the external geometric form and
24 internal arrangement and nature of storey contacts, a summary of which is given in Table 1. Five key

1 geometries; massive (M); semi-amalgamated (SA); internally amalgamated (IA); offset stacked (OS); and
2 isolated (I) were identified in the basin, with geometries M, SA, IA, and OS being subdivisions of the well-
3 known 'sheet' geometry (e.g. Friend et al., 1979).

4 **BIGHORN BASIN**

5 **Tectonic setting and basin extent**

6 The Bighorn Basin is a NNW–SSE trending basin situated in north-western Wyoming with its most
7 northerly extent residing in central-southern Montana (Fig. 1). Extensive exposure across a large portion
8 of the basin alongside an established chronostratigraphic framework thanks to extensive work on
9 mammalian fossils (Gingerich & Clyde, 2001), magnetostratigraphic control (Secord et al., 2006; Clyde et
10 al., 2007) and the presence of the Palaeocene–Eocene Thermal Maximum (PETM) (e.g. Baczynski et al.,
11 2013; Foreman, 2014; Kraus et al., 2015) makes the Bighorn Basin a good candidate basin for a basin-
12 wide study of continental deposits. As a result locations can be placed into particular portions of the
13 basin fill stratigraphy.

14 The Bighorn Basin is the product of a switch from thin-skinned Sevier (Late Jurassic – Palaeogene)
15 deformation to thick-skinned Laramide (Late Cretaceous – Early Eocene) deformation caused by north-
16 east to south-west shortening and segmentation of the Sevier foreland basin into more discrete basins
17 (Snyder et al., 1976; Dickinson et al., 1988; Decelles, 2004; Fan & Carrapa, 2014). Laramide-aged
18 basement cored uplifts define some of the Bighorn Basin margin, namely the Beartooth Range to the
19 north-west, the Owl Creek Mountains to the south and the Bighorn Mountains to the east (Fig. 1A).

20 The western to south-western limit of the Bighorn Basin is less well constrained as the mid to late-
21 Eocene Absaroka Volcanics, which form the Absaroka Mountains (Rouse, 1937), cover older successions
22 and structural features (Sundell, 1990). As a result, several different source areas to the west have been
23 proposed in the literature. The Cody Arch, which marks the extent of the present day Bighorn Basin, is

1 considered by Van Houten (1944) and Sundell (1990) to be the western edge of the basin, with a
2 distinctively different basin lying to the west of this structural feature (the Absaroka Basin of Sundell,
3 1990). Lillegraven (2009) discounts this based on detailed structural analyses in the Cody Arch area, and
4 instead proposes the Washakie Range (Fig. 1A) as the western source area for the basin. Kraus (1985)
5 also showed the Washakie Range as the western limit of the Bighorn Basin, but argued that the Basin
6 Creek uplift, situated in the southern portion of Yellowstone National Park (Fig. 1A), was a key sediment
7 source area. To the north, the Nye bowler lineament and Pryor Mountains (Fig. 1A) are considered to
8 have had topographic expressions during the Palaeocene–Eocene; however, they are not considered to
9 have been a consistent barrier to drainage (Dickinson et al., 1988) or to have been a significant sediment
10 source, as is shown by palaeocurrent data (Seeland, 1998) and similar aged deposits lying on top of the
11 lineament (Wilson, 1936). The northern extent of the Bighorn Basin in Montana is sometimes referred to
12 as the ‘Clarks Fork Basin’ in the literature (e.g. Hickey, 1980; Gingerich & Clyde, 2001; Kraus, 2001).

13 **Previous sedimentological work**

14 The Palaeocene Fort Union and Eocene Willwood formations are interpreted as the product of
15 meandering rivers, braidplain or alluvial fan channel and various floodplain deposits (e.g. Van Houten,
16 1944; Bown & Kraus, 1983; Bown & Kraus, 1987; Kraus, 1987; DeCelles et al., 1991; Willis &
17 Behrensmeyer, 1995; Kraus & Wells, 1999; Davies-Vollum & Kraus, 2001; Kraus, 2001; Kraus & Davies-
18 Vollum, 2004; Foreman, 2014), with minor amounts of lacustrine deposits which were deemed to be
19 shallow and of limited aerial extent also recognised (Hickey & Yuretich, 1997; Yuretich et al., 1984).
20 Many studies on the Fort Union and Willwood formations in the Bighorn Basin have concentrated on
21 documenting the detailed sedimentology at either a single, or a few selected outcrops within the
22 modern geographic extent of the basin. For example, DeCelles et al. (1991) document in detail the
23 coarse-grained deposits that lie adjacent to the Beartooth Mountains, while Kraus (1985) documents
24 conglomeratic deposits in the south-western portion of the basin. Others assess channel and floodplain

1 characteristics (e.g. Hickey, 1980; Willis & Behrensmeier, 1995; Kraus & Gwinn, 1997; Kraus, 2001), or
2 have focused on the superbly exposed palaeosols (e.g. Bown & Kraus, 1981; Bown & Kraus, 1987; Kraus,
3 1987; Kraus & Bown, 1993) or on aspect of avulsion deposits (Kraus, 1996; Kraus & Wells, 1999; Davies-
4 Vollum & Kraus, 2001; Kraus & Davies-Vollum, 2004; Jones & Hajek, 2007) and on the organic rich
5 deposits within the basin (Davies-vollum & Wing, 1998). Other studies have concentrated on deposits
6 associated with the Palaeocene–Eocene Thermal Maximum (e.g. Kraus et al., 2013; Foreman, 2014;
7 Kraus et al., 2015).

8 There are few sedimentological studies that have been conducted at or near the basin scale (e.g. Van
9 Houten, 1944; Neasham & Vondra, 1972; Seeland, 1998). Van Houten (1944) was the first to define the
10 Willwood Formation, and focused on presenting lithological descriptions of various outcrops around the
11 modern basin. Neasham and Vondra (1972) built upon this by conducting palaeocurrent, facies and
12 petrographical analyses of the Willwood Formation. However, both of these studies are restricted to the
13 Willwood Formation of what is considered the modern extent of the basin. Seeland (1998) extended his
14 study to both the Fort Union and Willwood formations, but focused on assessing palaeocurrent patterns
15 in the basin.

16 The aim of this study is to build upon previous work by conducting a study that extends beyond the
17 modern Bighorn Basin extent. It will integrate both the Fort Union and Willwood deposits as
18 palaeocurrent studies, a lack of evidence of any changes in source areas, and continuous gradual
19 sedimentation indicate the Willwood is a continuation of the Fort Union (Seeland, 1998), with a colour
20 change from drab-grey to red palaeosols distinguishing the two units lithostratigraphically (Willis &
21 Behrensmeier, 1995).

22 **RESULTS**

23 **Vertical trend analyses**

1 **Results**

2 The Bighorn Basin has an asymmetrical synclinal fill, resulting in exposures in the centre of the basin
3 being younger in age than those situated at basin margin locations (Gingerich, 1983; Kraus, 1992; Willis
4 & Behrensmeyer, 1995; fig. 25 of Finn et al., 2010). This has important implications for assessing the
5 spatial trends across the basin because deposits do not directly correlate from the basin margin to the
6 basin centre. It is important to consider any vertical trends as deposits may have formed under different
7 conditions through time, and therefore changes in deposit character may be the result of temporal
8 rather than spatial controls. To assess whether there were any substantial temporal changes in the
9 Palaeogene Bighorn Basin, an analysis of vertical trends was conducted. Due to exposure limitations a
10 combined sedimentary log of the Fort Union and Willwood deposits could not be constructed, therefore
11 an assessment of vertical trends was undertaken at two scales; firstly at a broader stratigraphic scale
12 whereby analysis of the deposits was undertaken in terms of comparison between the two formations,
13 and secondly at a smaller local scale where up-section trends were analysed within each vertical section
14 logged (ranging from 47 m to 500 m).

15 A change in the average channel body thickness between the Fort Union and Willwood formations is not
16 observed (Fig. 2A). Fort Union channel bodies have an average thickness of 7.6 m while Willwood
17 channel bodies have an average of 7.3 m. However, a difference in the maximum channel body
18 thickness measured for each formation is observed, with the Fort Union having a maximum channel
19 body thickness of 44.5 m and the Willwood 23.8 m (Fig. 2A). Similarly, the Fort Union has a relatively
20 high standard deviation (7.3 m) and a high coefficient of variance (99%), while the Willwood has a
21 comparatively lower standard deviation (4.3 m) and coefficient of variance (59%). A small degree of
22 variability in channel presence is observed between the Fort Union and Willwood formations as the
23 overall proportion of channel deposits is 33% for the Fort Union Formation, and 29% in Willwood
24 Formation. A change in the dominant channel body geometry type present from the Fort Union into the

1 Willwood is observed. The more amalgamated and coarser-grained channel body geometries (M and SA;
2 see Table 1) are only observed in Fort Union Formation (Fig. 2B), while the least amalgamated
3 geometries (OS and I; see Table 1), although not exclusive to the Willwood Formation, are more
4 prevalent in the Willwood than the Fort Union Formation.

5 An analysis at the local scale was also conducted (i.e. within each succession logged internally within the
6 formations ranging from 47 m to 500 m in thickness) to assess the presence of any smaller-scale trends.
7 Channel body thickness was plotted against height in the sedimentary succession, with the channel body
8 type also noted (Fig. 3). A ρ value (Spearman's rank correlation coefficient) and coefficient of variance
9 (CV) was calculated for each sedimentary succession, with associated moving averages plotted for the
10 variables height in succession versus channel-body thickness (Fig. 3A). The 28 studied sections can be
11 broadly characterised into several groups. The first group have ρ values of less than ± 0.19 representing
12 'very weak or no relationship'; the second group ± 0.2 to 0.39 (weak relationship); group 3 ± 0.4 to 0.59
13 (moderate relationship); group 4 ± 0.6 to 0.79 (strong relationship); and group 5 ± 0.8 to 1.0 (very strong
14 relationship). As can be seen in Fig. 3, there is no particular dominance in terms of number of sections
15 within a particular category with 7 out of 28 successions being present within the 'weak to no
16 relationship', 6 in the 'weak', 7 in the 'moderate', 5 in the 'strong' and only 3 in the 'very strong'
17 grouping, indicating there is no consistent increase, or decrease, in channel body thickness with height
18 in succession. Similarly, these groupings have no particular dominance in space with all groups being
19 observed across the basin and within different mammalian (NALMA) age intervals. Of those that are in
20 the 'moderate' to 'very strong' groupings, both negative and positive correlations can be seen, with
21 locations 12, 17, 21, 22, 25 and 26 showing negative correlations (i.e. decreases in channel body
22 thickness up-section), and locations 3, 4, 11, 14, 15, 19, 20, 27 and 28 showing a positive correlation (i.e.
23 increase in channel body thickness up-section). The coefficient of variance (ratio of the standard
24 deviation to the mean; CV) was also calculated for each succession. As can be seen in Fig. 3, a range of

1 CV values are present from 21% to 134%. A cumulative frequency plot of CV values (Fig. 3B) shows that
2 there are three groupings of CV values; Low (0 to 40%; 5 localities), moderate (41 to 70%; 15 localities)
3 and high (70 to 134%; 8 localities). With the exception of localities 5, 6, 10, 14 and 26, which lie in the
4 low CV category; channel body thickness is generally considered to vary relatively within each
5 succession. Low CV values are generally found to be present in the centre of the basin, although
6 moderate and high CV values are also present. High CV values are generally found to be present at basin
7 margin localities, but again moderate values can also be present in these locations.

8

9 ***Discussion of vertical trends***

10 The two scales of study conducted above have allowed valuable insights into the Palaeogene fill of the
11 Bighorn Basin to be gained. The maximum channel body thickness is considerably larger for the Fort
12 Union Formation (44.5 m) than the Willwood (23.8 m). This has also resulted in a difference in standard
13 deviation and CV (see Fig. 2) because these statistics are influenced by the maximum channel body
14 thickness. Although variation is observed between the two formations, this is considered to be largely a
15 function of where the two units are exposed. The Fort Union Formation is more exposed along the basin
16 margin, where larger more amalgamated geometry types would be expected, whereas the Willwood
17 Formation is more prevalent in the basin centre. However, when looking at the average channel body
18 thickness (7.6 m for the Fort Union Formation and 7.3 m for the Willwood Formation) and channel
19 presence (33% for the Fort Union Formation and 29% for the Willwood Formation) little difference is
20 seen between the two.

21 Although it is not within the scope of this paper to investigate the specific causes for the vertical trends
22 observed at each locality, it is important to note that such internal variations, and therefore local
23 controls, make the fill of the Bighorn Basin rather heterogeneous. As discussed above, channel body

1 thickness can increase, or decrease, up-section, or as is the case for those grouped into weak to no
2 relationship category, no systematic change in channel body thickness can also be observed. Up-section
3 changes whereby channel body thickness decreases, or increases, are indicative of a change in the
4 processes that affect fluvial channel characteristics and preservation. For example, up-section increases,
5 or decreases, in channel body thickness may be the result of downstream influences, such as
6 alternations in accommodation through base level or subsidence, or changing conditions upstream, such
7 as variations in sediment supply as a consequence of fluctuating climate (Shanley & McCabe, 1994;
8 Posamentier & Allen, 1999; Catuneanu 2006, Holbrook et al., 2006). Up-section increases in channel
9 body thickness may also be the result of the fluvial systems prograding through facies belt expansion or
10 entrenchment and bypass (e.g. Legarreta & Uliana 1998; Rittersbacher et al., 2014; Owen et al., 2017).
11 Similarly an up-section decrease in sandstone body thickness may be the result of retrogradation of a
12 system through time (e.g. Kukulski et al., 2013). For sedimentary successions in which only weak or no
13 correlations are observed, two deductions can be made. Firstly, that channel body thickness is relatively
14 consistent up-section. Examples of this include localities 5, 6 and 10 (Fig. 3B) whereby channel body
15 thickness does not considerably change up-section and low CV values are observed. In such cases it is
16 inferred that the fluvial conditions are similar through time (e.g. Nichols & Fisher, 2007). The second
17 deduction for a lack of correlation is that there is a high degree of variability with regards to channel
18 body thickness up-section. Examples of this include localities 1, 16, 23 and 24 where low ρ values ($<\pm 0.4$)
19 are observed alongside high CV values (i.e. $>70\%$). In such instances, it is inferred that there are abrupt
20 changes in important boundary conditions, such as sediment supply, climate (i.e. associated with the
21 PETM, e.g. Foreman et al., 2014) or accommodation/base level (i.e. possible changes in base level
22 associated with nearby lakes (Yuretich et al., 1984), that are forcing the channels to become abruptly
23 thinner/thicker over relatively short intervals. As noted above, the highest CV values are generally
24 present at the basin margin, and low CV values in the basin centre. It is suspected that this is because

1 the fluvial systems are less susceptible to up-stream changes such as sediment supply and discharge
2 variations when compared to basin centre locations.

3 The temporal changes identified here need to be taken into consideration when analysing spatial trends
4 across the basin as it should be noted that younger Willwood Formation deposits mainly reside in basin
5 centre locations, and that older Fort Union deposits are restricted to basin margin locations (Fig. 1). This
6 means that these locations cannot in the strictest sense be assumed to be directly comparable;
7 however, the above analyses shows that no major shift is observed between the two formations, just
8 internal local (quite possibly autocyclic scale related to avulsion cycles) variations are observed,
9 therefore allowing the spatial comparison to be conducted with a degree of confidence. Vertical
10 changes in the basin-fill of the Bighorn Basin were also identified by Neasham & Vondra (1972) who
11 interpreted a decreasing stream gradient through time during the Willwood Formation. Other workers
12 have identified an overall change in palaeosol character from relatively drab grey soils in the Fort Union
13 to dryer red soils in the Willwood Formation, which is deemed to be result of improved drainage
14 conditions through and/or a change to warmer and drier conditions (e.g. Gingerich, 1983; Willis &
15 Behrensmeyer, 1995; Kraus et al., 2013).

16

17 **Spatial analyses**

18 ***Palaeocurrent analyses***

19 Palaeocurrent directions were measured and combined from cross-bedding and imbricated clasts within
20 channel deposits to produce the palaeocurrent map (Fig. 4A). A broadly north-east direction can be
21 observed in the basin, within which several principal source areas can be defined. The Beartooth
22 Mountains in the north-west of the basin are an obvious source area, with flow heading east into the
23 centre of the basin (herein referred to as the Beartooth systems). Dispersion of palaeoflow within the

1 Beartooth systems is deemed to be the result of multiple point-sourced fluvial systems entering the
2 basin from the Beartooth Mountains, as has been documented by DeCelles et al. (1991). An additional
3 source area to the west (herein referred to as the Absaroka system) can be deduced from palaeocurrent
4 data at locations 12 and 23 (Fig. 4A). Deposits at these locations are interpreted to represent a separate
5 system to the Beartooth systems as the sites are situated further west and south of the Beartooth
6 Mountains (Fig. 1). The Owl Creek Mountains and an additional source area to the south-west, now
7 occupied by the Mid–Late Eocene Absaroka Volcanics, is inferred from palaeocurrent data in the
8 southern portion of the basin. Specific entry points are difficult to define in the southern portion of the
9 basin as palaeocurrent directions gradually change from north to north-east to true north from west to
10 east along the basin margin. An axial system can be defined in much of the basin centre with average
11 flow going in a north to north-east direction, perpendicular to the lateral inputs of the Beartooth and
12 Absaroka systems (Fig. 4A). However, an overall north to north-east palaeocurrent direction in the far
13 north suggests that the axial system was being diverted, most likely due to interaction with deposits of
14 the Beartooth systems, rather than following the north-west trending basin axis (Fig. 4A). From this
15 dataset alone it is not possible to define how the axial system relates (i.e. is the downstream extent) to
16 systems being sourced from the south.

17 Palaeocurrent data and interpretations presented here are in broad agreement with those of Neasham
18 & Vondra (1972) and Seeland (1998), with the exception of the influence of the Bighorn Mountains to
19 the east. Neasham & Vondra (1972) suggest that major drainage networks were sourced from the
20 Bighorn Mountains. However, the palaeocurrent data here (Fig. 4A) do not support this interpretation
21 indicating flow to the north to north-east, parallel to the Bighorn Mountains rather than away from
22 them. The absence of an easterly derived drainage system preserved within the present day basin-fill,
23 suggests that either easterly-derived fluvial systems were relatively small and have been removed by

1 erosion or that the Bighorn Mountains were not of sufficient elevation to source systems into the basin,
2 but were capable of diverting flow northwards (Seeland, 1998).

3 ***Weighted average grain-size of channel deposits***

4 A weighted average grain size rather than a simple average, was calculated at each location so that the
5 thickness of the channel deposits was taken into account (e.g. Owen et al. 2015). This was achieved by
6 taking the model grain size from each bed that was interpreted to be part of a channel fill (i.e. decimetre
7 to metre-scale). In the case of mudstones, a value of 0.0156 mm (silt) was taken based on the more
8 prevalent silt content within the channel fills. Key sediment source areas defined from palaeocurrent
9 data can also be recognised in this grain-size dataset (Fig 4B). Conglomeratic grain-sizes along the
10 Beartooth Mountain front support the interpretation that this area was an important sediment source.
11 A drop in grain size in the most northern location (location 4, Fig 4B) in comparison to other Beartooth
12 margin locations suggests that either this location captured the along strike distal fringes of a fluvial
13 system, or that the sediment calibre of this system was distinctively different in comparison to the other
14 Beartooth systems. The Absaroka system to the west is also evident in the grain-size dataset where
15 average grain sizes are slightly coarser (0.37 and 0.43 mm at sites 12 and 23, respectively, Fig. 4B), than
16 at basin centre locations (0.11 mm). However, channel deposits in the Absaroka systems are finer
17 grained than the Beartooth systems, either implying a different catchment geology and sediment calibre
18 or that the source area for the Absaroka systems was much further to the west. Systems to the south
19 can be better constrained using the grain-size dataset, as a conglomeratic input is evident in the south-
20 western portion of the basin (herein referred to as the Washakie system, Fig. 4B), while a finer grained
21 input (medium to very fine sandstone) is more evident from the south (herein referred to as the Owl
22 Creek systems, Fig. 4B). An eastern input is also not evident in the grain-size dataset.

1 Using the palaeocurrent dataset to establish stream flow direction, an analysis of downstream trends
2 can be conducted on the grain-size dataset. A clear decrease in grain-size can be observed from the
3 Beartooth systems, into the axially flowing central system in the northern portion of the basin. The
4 generally consistent grain-size along strike of the northern portion of the axial fluvial system suggests
5 that the Beartooth systems did not provide any significant contribution of coarse material into the axial
6 fluvial system, at least during the Eocene as the deposits furthest to west are considered to be
7 Wasatchian ages 1 to 4 (Early Eocene), and do not show any coarsening towards the Beartooth systems
8 (Fig 4B). A general decrease in grain-size can be seen in the Absaroka and Owl Creek systems and the
9 northern portion of the Washakie system. The axial system gradually increases in grain size downstream
10 as it passes the Washakie and Absaroka lateral inputs until the northern portion of the basin (from silt
11 sizes to medium sand to conglomerate sizes), after which a drop in grain size is observed in the very far
12 north (from very fine to medium sand) (Fig. 4B). This suggests that the axial fluvial system experienced
13 increased sediment input and/or increased downstream sediment transport capacity until north of the
14 Beartooth systems. A decrease in grain-size is also not present in the southern portion of the Washakie
15 system where sandstones grade into conglomerates downstream. However, beyond this point a
16 downstream reduction can be seen (Fig. 4B).

17 It should also be noted that an alternative interpretation related to temporal and spatial trends could be
18 put forward, with the basin margin to basin centre trends representing fining of the channel deposits
19 through time as basin centre deposits are generally younger than those on the margin. This is also true
20 for the axially flowing system as deposits in the south are finer, and of a younger age, than those
21 situated in the northern portion of the basin centre.

22 ***Channel body percentage***

1 The percentage of channel facies present in logged sections was calculated to assess variability in
2 channel deposit proportions across the basin. Covered sections were avoided in most instances, but
3 when they could not be they were assumed to be finer grained floodplain deposits, which was often
4 clarified lateral to where logs were taken. In total, channel deposits comprised 34% of total sediment
5 logged. However, as can be seen in Fig. 4C, channel proportion is highly variable across the basin varying
6 from 12 to 81% of the successions logged. In general the highest channel percentages are observed on
7 the western margin of the basin, and lowest in the basin centre. Downstream trends are largely in
8 agreement with those depicted from the grain-size dataset, with a general downstream reduction in
9 channel-body percentage being observed in the Beartooth, Absaroka and Owl Creek systems (Fig. 4C).
10 Downstream increases, as seen in the grain-size dataset, are also observed in the axial system. An
11 increase in channel proportion is seen from south-east to north-west until the Beartooth systems have
12 been passed, after which there is a reduction. The Washakie systems, however are highly variable with
13 an initial decrease then increase being observed in the northern portion, while an increase and then
14 decrease is observed in the southern portion.

15 Although these broad trends can be recognised, spatial variability can be observed within the
16 documented systems. For example, in the Beartooth systems channel deposits compose up to 81% of
17 the succession but can also be as low as 12% between different sections (Fig. 4C). Within the northern
18 portion of the axial system a high degree of variability is also observed across depositional strike ranging
19 between 18% and 48% of the deposits logged (noted in Fig. 4C). Although locations in this region are
20 assigned different mammalian ages, temporal variations cannot account for the variability in channel
21 percentage as locations with the same mammalian age are still highly variable. For example channel
22 deposits with a Clarkforkian age vary in proportion from 18 to 34% (Fig. 4C).

23 As with the grain-size dataset, care must be taken in assuming the described trends solely relate to
24 spatial variations as channel presence is commonly lowest in the youngest (southern basin centre)

1 sections which are Willwood in age. However, as the vertical trend analyses showed there is no
2 substantial change in channel proportion overall between the datasets for the two formations, it is
3 deemed that a spatial cause can be inferred.

4 ***Channel-body thickness trends***

5 Three quantities were used when analysing the thickness of channel deposits: average channel-body
6 thickness, maximum channel-body thickness and average storey thickness, Fig 4D to F). These values
7 represent the descriptive statistics for the true thickness of channel-bodies measured at each section. As
8 can be seen in Fig. 4D, the highest average channel-body thicknesses are generally situated at basin
9 margin locations within the Beartooth, Absaroka and Washakie systems, and the lowest in basin centre
10 locations, although anomalies are present (for example, location 2 in the Beartooth system, Fig 4D). The
11 range in average thicknesses is large across the basin, ranging from 4 to 20 m. Downstream decreases in
12 average channel body thickness are evident from all four interpreted source terrains, apart from the
13 northern portion of the Washakie system which decreases and then increases downstream. As with
14 other datasets, the axial system increases in thickness downstream, with the northern portion of the
15 centre of the basin having relatively high average thicknesses (Fig. 4D).

16 The range in maximum channel-body thicknesses is also large, ranging from 6 m to 48 m (Fig. 4D). The
17 largest maximum channel bodies are generally situated at basin margin locations, and lowest in the
18 basin centre (Fig. 4D), although locality 2 is again anomalous as it is only 4 m there. Downstream
19 decreases in maximum channel-body thickness are evident when averaged over the area for the
20 Beartooth and Absaroka systems into the axial system. Within the Washakie and Owl Creek fluvial
21 systems variable trends are observed. In the Washakie system a downstream decrease and then
22 increase in channel-body maximum thickness is observed in the northern portion of the system, while a
23 downstream increase is observed in the southern part of the system (Fig. 4D). Similarly, the western

1 portion of the Owl Creek system shows a decrease in maximum channel thickness, and the eastern
2 portion increases in thickness downstream. Finally, a downstream increase in thicknesses is observed in
3 the axial fluvial system (Fig. 4D).

4 The range in average storey (defined as the erosional surface of the active portion of a channel base,
5 that incises into previous channel deposits, Owen et al. 2017) thicknesses is much less than for mean
6 and maximum channel-body thickness datasets with average storey thicknesses ranging from 3 m to 10
7 m (Fig. 4F). The majority of the highest values are present at basin margin locations and lowest values at
8 basin centre locations, however this trend is not as evident as that of other thickness datasets due to
9 the low range in thicknesses involved. When analysing downstream trends in average storey thickness
10 within the defined systems, downstream decreases can be identified in the Beartooth and Absaroka
11 systems into the axial system, whereas a downstream increase in storey thickness is observed in the Owl
12 Creek system (Fig. 4F). Again variable trends are observed in the Washakie system with the northern
13 portion displaying an initial decrease and then increase in average storey thickness, while the southern
14 portion shows a decrease. In the Owl Creek system the smallest average storey thickness is found on the
15 basin margin (3 m), which then increases in thickness into the centre of the basin, after which no trends
16 can be identified as thicknesses are relatively uniform until the most northern locality (Fig. 4F). It is
17 speculated that the smaller range in storey thickness, and apparent dampening of downstream trends in
18 comparison to the average channel body and maximum channel body thickness datasets implies that
19 there is increased stacking of storeys at the basin margin relative to the basin centre. With this in mind it
20 can be inferred that there were relatively uniform rates of down-cutting of the river channels and
21 subsequent preservation of the deposits in order to produce the observed small range in storey
22 thicknesses, because if this were not the case a high range would be observed.

23 Overall, the different thickness statistics of channel deposits demonstrate how highly variable the fluvial
24 systems within the Bighorn Basin are. Some of the predicted generic trends can be observed, such as the

1 thickest deposits generally residing in basin margin localities, or general downstream decreases in
2 average and maximum channel-body thickness, as well as storey thickness for the Beartooth and
3 Absaroka systems into the axial system. Trends are not evident, or consistent, in the Washakie, Owl
4 Creek and axial fluvial systems for the three different thickness statistics.

5 ***Channel-body type (geometry) trends***

6 Owen et al. (2017b; Fig. 12) documented the proportion of each channel-body type (geometry) in each
7 of the studied sedimentary successions in the Bighorn Basin and showed that sedimentary successions
8 are commonly composed of several different geometry types. These authors showed that the more
9 amalgamated geometries (M and SA) are only found near basin margin locations, geometries OS and I
10 are found across the sedimentary basin, but are most prevalent in basin centre locations, while
11 geometry IA can be found across the whole basin. A more detailed analysis of the geometries can be
12 conducted by assessing their spatial variability within the four systems delineated within this paper.
13 Figure 5A summarises the dominant geometry at each location in the basin, based on data presented in
14 Owen et al. (2017b), and shows how highly variable the four systems are in relation to one-another (Fig.
15 5A). The Beartooth systems are dominated by geometry SA, while the Absaroka systems are dominated
16 by the less amalgamated geometry IA. The Owl Creek systems are dominated by geometry IA at basin
17 margin locations, yet change quickly downstream to the lesser amalgamated geometry I (Fig. 5A). The
18 deposits of the Washakie and axial fluvial systems are highly variable, with multiple different geometries
19 found within these systems (Fig. 5A). The Washakie system in its most proximal locations is dominated
20 by Geometry IA, yet further downstream it is composed of M and SA geometries, whereas the axial
21 system is composed of geometry I in its upstream extremities until it is laterally equivalent to the
22 Absaroka system, where it changes to being dominated by geometries OS, IA and I.

23 **DISCUSSION**

1 **Characterising the fluvial systems**

2 It was hypothesised from modern-day studies (e.g. Weissmann et al., 2010; 2015) that distributive fluvial
3 systems (DFSs) should form important components of ancient sedimentary basin fills. Distributive fluvial
4 systems have been shown from previous work to have predictive downstream trends with a
5 downstream decrease in channel proportion, amalgamation and size, as well as a decrease in overall
6 grain size in the succession (e.g. Friend & Moody-Stuart, 1972; Hirst, 1991; Kelly & Olsen, 1993;
7 Weissmann et al., 2010, 2013, 2015; Owen et al., 2015; Cain & Mountney, 2011). However, deposits
8 associated with incisional river valleys are expected to have large-scale incisional surfaces and an
9 associated interfluvial palaeosol (McCarthy & Plint, 1998). It is also expected that these systems will not
10 show downstream decreases in associated characteristics (i.e. increase in channel size and
11 amalgamation downstream) due to tributary networks joining the trunk system (e.g. Weissmann et al.,
12 2010, 2015). As can be seen in Table 2, downstream decreases in grain size, channel proportion, average
13 and maximum channel-body thickness, average storey thickness and a change to less amalgamated
14 geometries can be observed in the Beartooth and Absaroka datasets, indicating the systems are
15 distributive in nature, as is to be expected. As can be seen with the palaeocurrent data (Fig. 4A) an
16 overall larger (i.e. basin-scale) tributary pattern is observed as the different systems merge and
17 contribute to the axial systems (i.e. contributory pattern of Hartley et al. 2010). DeCelles et al., (1991)
18 also interprets the Beartooth systems to be composed of multiple alluvial fans and a braid plain deposit.
19 The Owl Creek systems do show a downstream decrease in grain size, channel proportion, average
20 channel body thickness and amalgamation. However, an increase in storey size is observed alongside a
21 variable maximum channel–body thickness distribution. Despite this discrepancy, the Owl Creek systems
22 are however still considered to be distributive in nature because evidence for them being tributary (i.e.
23 through the presence of significant erosional surfaces, mature interfluvial palaeosols and a tributary
24 palaeocurrent network) are not observed in the deposits.

1 In contrast, the Washakie and axial fluvial systems do not show downstream trends associated with DFS
2 deposits. For a considerable portion of the axial system a downstream increase in grain size, channel
3 body thickness and presence is observed, alongside a change in geometry to more amalgamated forms
4 (see Figs 4 and 5; Table 2), the opposite of which would be expected for a DFS. Interestingly, this is
5 concurrent with the transverse systems (for example, Washakie, Absaroka and Beartooth) entering the
6 basin centre. As can be seen in Fig. 4 the transverse systems are larger and coarser grained than those of
7 the Owl Creek systems – the upstream portion of the axial system. As would be expected, downstream
8 predicted DFS trends are not observed in the axial fluvial system due to the introduction of the larger,
9 coarser grained transverse systems, resulting in an increase in discharge and sediment load into the axial
10 fluvial system. It is not until the Beartooth systems, the most northerly transverse systems, are
11 geographically passed to the north that downstream trends are observed. More localised studies
12 conducted on the axial fluvial system by Kraus & Wells (1999) and Jones & Hajek (2007) show the system
13 to be dominated by avulsion processes. These studies together with a lack of interfluvial palaeosols and
14 significant channel incision indicate that the axial system was not held in a river valley and therefore was
15 relatively unconfined in nature as the basin became filled through time. The transverse systems were
16 not large enough to ‘pin’ the axial fluvial system against the Beartooth Mountains, but entered the basin
17 centre from the west and joined the axial system in a contributory nature (Fig. 5D), which possibly
18 implies that the basin was under-filled. Axial system morphology has been shown in physical laboratory
19 based experiments (Experimental EarthScape basin) by Connell et al. (2012a,b) to be greatly influenced
20 by transverse system dynamics. These studies provide a laboratory based controlled example of where
21 the transverse systems are not large enough, possibly due to a lack of effective discharge or slope, to
22 confine the axial system. The present study provides a rock record example of an axial fluvial system
23 that is unconfined in nature, such as the Rio Mimbres (Mack et al., 1997), and that not all basins may

1 have a confined axial system unlike modern examples in some ancient basin studies (e.g. Kukulski et al.,
2 2013; Lawton et al., 2014).

3 The deposits of the Washakie systems show more variation than that of the axial system. Downstream
4 trends are difficult to identify and when present downstream decreases and increases are observed
5 within the different datasets (Figs 4 and 5). Using the data maps presented, no plausible
6 sedimentological explanation is proposed to explain the complex nature of the system. However, field
7 observations and work by Van Houten (1944) indicate that an angular unconformity is present at
8 Location 20 (Fig. 1B). As can be seen in Fig. 6D, this angular unconformity is very pronounced with
9 dipping fine-grained Fort Union Formation deposits overlain by flat-lying conglomeratic Willwood
10 Formation deposits. Fort Union Formation deposits have been mapped further west of this location (Fig.
11 1B), suggesting that the unconformity resulted from syn-depositional intrabasinal thrusting, which
12 would have disrupted any associated downstream trends.

13 Based on the degree of amalgamation and spatial distribution of the channel-body types (geometries) in
14 the Bighorn Basin, it was inferred by Owen et al. (2017b) that the identified channel-body types could lie
15 on a continuum, and reside within specific portions of a distributive fluvial system (DFS). It may
16 therefore be possible to infer the position where each location resides on a DFS based on the dominant
17 geometry present. Figure 5B illustrates the interpreted DFS position for each location, with locations
18 dominated by M representing a proximal location, SA proximal-medial, IA medial, OS medial-distal and I
19 distal locations. As can be seen in Fig. 5B, deposits in the Beartooth systems are interpreted to represent
20 proximal–medial localities, which downstream pass into medial to distal deposits of the axial system,
21 showing predicted DFS trends. Similarly downstream predicted trends can be observed in the Absaroka
22 system where deposits are interpreted to be medial DFS deposits, which downstream grade into medial-
23 distal deposits in the axial fluvial system (Fig. 5B). The fact that these deposits are interpreted to be
24 medial further supports interpretations from other datasets that the source area for the Absaroka

1 systems must have been located much further to the west of the current basin margin. Broad
2 downstream trends can also be observed in the Owl Creek systems where interpreted medial and
3 medial–distal deposits change to distal deposits downstream (Fig. 5B).

4 Predicted downstream DFS trends are not apparent in the Washakie or axial fluvial systems (Fig. 5B).
5 Again, variable trends are present in the Washakie system with the northern portion showing predicted
6 downstream trends (proximal–medial to distal), whereas the southern portion of the system does not
7 (medial to proximal–medial deposits downstream trend), with interpreted proximal deposits separating
8 these two areas. The axial system shows reverse DFS trends for much of its length as it moves
9 downstream from interpreted distal deposits to medial to distal deposits, with variability being evident
10 along strike in the northern portion of the system (Fig. 5B). It can therefore be seen that this method of
11 inferring proximity can only be applied successfully to a certain extent. This suggests that either the DFS
12 model cannot be applied effectively to the Bighorn Basin, or that the method of using dominant
13 channel-body type to infer DFS position is not significantly robust as changes in channel body geometry
14 may arise from other controlling factors such as sediment supply or climate (Shanley & McCabe, 1994;
15 Posamentier & Allen, 1999; Catuneanu 2006, and Holbrook et al., 2006). Alternatively it could mean that
16 the concept can only be applied in discrete portions of the Bighorn Basin that represent DFS deposits as
17 opposed to those that represent axial fluvial systems. To assess which of these interpretations is correct,
18 other parameters (for example, channel proportion) for inferring location on a DFS need to be assessed.

19 The combined percentage of amalgamated geometries within each succession was also assessed, as
20 rock record studies have shown that this is useful in predicting downstream trends of DFS (e.g. Friend &
21 Moody-Stuart, 1972; Hirst, 1991; Kelly & Olsen, 1993; Owen et al., 2015). The deposits in the Bighorn
22 Basin have been characterised as being either proximal, medial or distal DFS deposits in Fig. 5C, based
23 on quantitative information derived using the Salt Wash DFS as an analogue because it is the only fully
24 quantified rock record example described to date (i.e. amalgamated channel percentage is 50% in

1 proximal deposits, 20 to 40% in medial, and <20% in distal locations, see Owen et al., 2015 for further
2 details). Data from Fig. 4C cannot be directly used as this dataset includes amalgamated and single
3 storey channel-body types. Therefore, the data in Fig 5C represent the percentage of all amalgamated
4 channel-body types (M, SA, IA and OS) to ensure that a direct comparison to Salt Wash data can be
5 achieved.

6 Important but subtle differences exist between the interpretations presented in Fig. 5B compared to Fig.
7 5C. Firstly, two sites in the Beartooth systems have been interpreted as comprising proximal deposits,
8 while location 4 (red d in Fig. 5C) has been interpreted as representing distal deposits. This discrepancy
9 highlights the importance of looking at multiple datasets, such as channel proportion and grain size, to
10 assess fluvial deposits as, although the dominant channel-body type suggests a proximal–medial locality,
11 channel deposits only account for <20% of the succession. It is suggested that the difference at location
12 4 is the result of the log sampling a distal alluvial fan system. Interpretation of these deposits as of a
13 medial position is consistent across the two datasets in the Absaroka system; however downstream DFS
14 trends are not evident in the amalgamated geometry percentage dataset as medial deposits still occur
15 downstream, again showing subtle but important differences between localities. The Washakie system
16 still shows a split in the northern and southern portion, but downstream DFS trends are evident. In the
17 northern portion, proximal through to distal downstream transitions can be observed, while in the
18 southern portion of the system medial through to distal transitions can be observed (Fig. 5C). This
19 indicates firstly that the same channel-body type is observed, but in different proportions, and also that
20 most proximal deposits in the southern portion of the Washakie system have not been sampled in this
21 study. Consistency is found between the two datasets in the Owl Creek and axial fluvial systems where
22 predicted medial down to distal transitions can be observed in the Owl Creek system, while trends not
23 consistent with the DFS model can be observed in the axial system (distal through to medial transitions)

1 (Fig. 5C). Overall, the datasets on amalgamation and spatial distribution of the channel-body types do
2 broadly align, but the subtle differences do highlight the highly variable nature of the deposits.

3 **Variability across the basin**

4 To highlight the variability within the basin-fill and how it is associated with the different systems,
5 example images (Figs 6 and 11) and four cross-sections have been produced (Figs 7, 8, 9 and 10). West–
6 east cross-sections were constructed for the northern (Fig. 7) and southern (Fig. 8) portions of the basin.
7 As can be seen in Figs 7 and 8, variability in channel-body type and channel proportion are generally
8 closely aligned to the different systems defined in the basin. For example, the Beartooth and Washakie
9 transverse systems are both noted in the west of the cross-sections by their relatively higher channel
10 proportion (53.0% and 45.5%, respectively) and dominance of more amalgamated channel-body types,
11 whereas the axial system has a lower channel presence (averages of 30.1% in the north and 20.3% in the
12 south) and channel-body types are less amalgamated. A higher degree of variability in channel-body
13 types, grain size and channel proportion in the axial system is present in the northern portion of the
14 basin (Fig. 7) compared to the south (Fig. 8). As noted previously, this variability is not deemed to reflect
15 temporal changes, as sections with the same mammalian age show variable channel-body type, grain
16 sizes and channel proportion. The relatively uniform grain size (Fig. 4B) and channel-body types in the
17 north (Figs 5A and 7) suggest that this variability may be associated with some sections capturing slightly
18 larger, better sorted, trunk rivers compared to the south. This may also be associated with the fact that
19 the northern portion is situated downstream of where the transverse systems enter the basin, whereas
20 the southern portion has less input from transverse systems. The inconsistency may therefore be
21 associated with variability related to variations in discharge and sediment delivery from these systems,
22 possibly associated with tectonic activity or changes in climate.

1 The north–south cross-section on the basin margin (Fig. 9) clearly shows the difference in nature
2 between the Beartooth and the Absaroka systems, as the Beartooth channel bodies are dominated by
3 coarse-grained more amalgamated channel-body types indicative of ephemeral alluvial fan deposits
4 (DeCelles et al., 1991) (Fig. 6A), whereas the Absaroka channel-bodies are more characteristic of a more
5 perennial amalgamated meander belt deposits (Hartley et al., 2015) (Fig. 6B and C). Interestingly,
6 variability internally within the Beartooth systems is evident, as the different logs transect different
7 parts [i.e. the core (location 1, Fig. 6A) and fringes (location 2)] of different alluvial fans that are
8 described by DeCelles et al. (1991). Identifying the Washakie and Owl Creek systems from the basin
9 margin cross-section is more challenging. Channel proportion does not allow the two systems to be
10 differentiated because proportions are fairly uniform along this portion of the basin margin. However,
11 when integrating more datasets the Washakie system can be identified as it is composed of more
12 amalgamated channel-body types (Fig. 9) and has a coarser grain size (Fig 4B). A cross-section spanning
13 south–north through the centre of the basin dissects the axial system of the basin. As can be seen in Fig.
14 10, a relatively high channel percentage is observed in the Owl Creek system (49%), after which a
15 reduction in channel proportion and change to less amalgamated channel-body types occurs, adhering
16 to the DFS model (location 26). However from location 26 though to 14, a downstream increase in
17 channel presence and a change to more amalgamated channel-body types is observed (Figs 10 and 11)
18 and this is defined here as being the transition point from the Owl Creek system into the axial system
19 and the result of laterally inputting transverse systems contributing into the axial system.

20 **Palaeogeographic model**

21 The presented datasets show the Palaeogene fill of the Bighorn Basin to be complex, with channel
22 proportion, channel-body types, grain size and channel body thickness varying greatly across the basin
23 (Figs 4 and 5). At face value, deposits appear to have an apparently random distribution in which order is
24 difficult to identify. However, by taking a systems rather than a lithostratigraphic approach and carefully

1 considering individual datasets and integrating information, five principal systems (Beartooth, Absaroka,
2 Washakie, Owl Creek and axial) can be identified. As can be seen in the presented datasets (Figs 4 and
3 5), these systems differ in size and character. Variation associated with the multiple different systems
4 gives rise to the complicated nature of the Fort Union and Willwood formations. A palaeogeographic
5 model for the Bighorn Basin during the Palaeogene is presented in Fig. 12. The axial system is an
6 important component of the depositional model, with the Beartooth, Absaroka, Washakie and Owl
7 Creek systems entering from various basin margin locations. Although not directly observable, it is
8 possible that systems could have been sourced from the Bighorn Mountains to the east, but were later
9 removed by erosion. However, if these systems were present it is clear that they were relatively minor in
10 size as limited influence or contribution from the east is observed in the axial system deposits.

11 The source areas for the Beartooth and Owl Creek systems are identified as being the Beartooth and
12 Owl Creek Mountains, respectively, which were present during the Palaeogene (e.g. Decelles, et al.,
13 1991; Seeland, 1998; Kraus, 2001). However, identification of source areas for the Absaroka and
14 Washakie systems is challenging due to exposure limitations. Kraus (1985) suggested that the
15 conglomerate deposits of the Washakie system were sourced from the north-west from the Basin Creek
16 Uplift, situated in southern Yellowstone National Park (Fig. 1A). However, this study offers an alternative
17 based on the identification of multiple different systems within the stratigraphic units. Firstly, as
18 highlighted in Fig. 4B, the Washakie system is considered to be relatively coarse-grained, with mean
19 channel grain sizes ranging from 1.07 mm (very coarse sand) to 2.97 mm (granule), suggesting a
20 relatively proximal location, close to the mountain front. As shown by Dingle et al. (2017) in a study of
21 the Himalayan foreland, the gravel–sand transition occurs on the fluvial systems, at most, 45 km from
22 the mountain front. These systems are considered to be substantially larger in size than those of the
23 Bighorn Basin, and therefore a distant source area, such as the Basin Creek Uplift, is unlikely. The
24 authors hypothesise, based on facies evidence and palaeocurrent data (Figs 4 and 5) that the Washakie

1 coarse-grained systems were sourced from the south-west, possibly from the Washakie Ranges or on
2 the western limit of the Owl Creek Ranges (Fig. 1A). The presence of the Absaroka system, which is
3 characterised by more medial deposits, also provides further evidence against a southern Yellowstone
4 source, because the Washakie system would need to cut through the Absaroka system to deposit the
5 conglomerates in their present position. Palaeocurrent data from the Absaroka system indicate a west
6 to north-west source area. The deposits of the Absaroka systems are deemed to represent medial DFS
7 deposits (Fig. 5B and C) and therefore, based on the interpreted position these deposits lie, it is
8 speculated that the Absaroka system was sourced in the vicinity of the southern portion of Yellowstone
9 National Park to the Jackson Hole/Teton Mountains area, such as from the Basin Creek Uplift or the
10 hypothetical Targhee Uplift (Fig. 1A).

11 **Spatial versus Temporal Trends**

12 The palaeogeographic model presented here represents an overview of the Palaeogene fill of the
13 Bighorn Basin. It is fully acknowledged that the fill of the Basin is asymmetrical, and therefore the
14 studied exposed portion of the fill does not directly correlate across the basin as basin centre deposits
15 are younger in age than basin margin deposits. Therefore, this study describes 'snapshots' of the
16 stratigraphy, and deposits may vary below and above the described sections. The vertical trend analyses
17 presented in this investigation shows that of the deposits studied, channel size and percentage do not
18 vary significantly from the Fort Union to the Willwood Formation but that a slight change to less
19 amalgamated forms from the Fort Union into the Willwood Formation is observed. However, it is argued
20 that the spatial trends described in this paper can be observed within deposits of similar age. For
21 example, as can be seen in the correlation panel presented in Fig. 11, the described downstream
22 increases in channel amalgamation and percentage occur within the same mammalian age (Wa-6 to Wa-
23 7). The authors do not discount that there may be elements of temporal change occurring in the basin,
24 particularly related to tectonic activity, as is evident by the presence of unconformities, and to a general

1 drying from the Palaeocene into the Eocene (e.g. Kraus & Middleton, 1987). It is plausible that systems
2 may have expanded and contracted in relation to autogenic and allogenic influences through time.
3 However, despite these temporal influences it is considered that the depositional model presented here
4 is a relatively robust representation of the different fluvial systems that occurred within the basin
5 throughout the Palaeogene.

6 This study outlines a predictive model that allows petroleum geologists to discern fluvial systems and
7 predictive trends at a variety of scales within lithostratigraphic units, with important implications for
8 reservoir identification and predictability at the exploration and production stages in subsurface
9 examples where significant levels of heterogeneity are observed across the basin.

10

11 **CONCLUSIONS**

12 This paper quantitatively documents the nature of a basin fill in which a physical stratigraphic rather
13 than a lithostratigraphic approach has been adopted, based on observations from modern basins. As has
14 been shown, the fill of the Bighorn Basin is complex; however, after careful analysis and integration of
15 multiple datasets it can be seen that a predictive framework can be developed that may be applicable to
16 other basins. Channel percentage and geometry type data sets were found to be particularly useful in
17 delineating the individual systems. The complex nature of the Bighorn Basin fill is shown to be directly
18 related to the different nature of the component depositional systems with a relatively wide axial
19 system and transverse distributive fluvial systems being identified. This study demonstrates that the
20 distributive fluvial system (DFS) concept can be a valuable model within which to decipher a relatively
21 complicated basin fill. It does however highlight that the axial system may not necessarily possess the
22 same down-dip trends as predicted in the DFS model, largely due to transverse system input along its
23 length. In this respect an overall tributary configuration is present at the basin scale, but it is imperative

1 to stress that the individual components are largely DFS in nature. The authors consider that predictive
2 models can be observed at two scales in this study: (i) at the system scale where predicted downstream
3 DFS trends are observed; and (ii) at the basin scale where the different, discrete geomorphic elements
4 can be identified. This largely concurs with observations from modern studies. The authors fully
5 acknowledge that other basins will vary with respect to the nature of an axial system (confined or
6 unconfined), or that there may be significant non-fluvial components such as aeolian or lacustrine
7 deposits in the basin. Combined with modern day studies this paper is considered to provide a step
8 forward in producing a framework for predicting facies and architectural variabilities for continental
9 basins

10 **ACKNOWLEDGEMENTS:**

11 This work was supported by Phase 2 of the Fluvial Systems Research Group (BP, BG, Chevron,
12 ConocoPhillips and Total). AE thanks the University of Aberdeen for additional funding and MGMS
13 thanks the São Paulo Research Foundation (FAPESP 2014/13937-3). The authors also wish to thank
14 numerous residents of the Bighorn Basin for their kind hospitality and access to land and Isobel
15 Buchanan and Alistair Swan for assistance in the field. The authors also thank reviewers Luca Colombera
16 and Sian Davies-Vollum and AE Christopher Fielding for helpful comments on this manuscript.

17

1 **FIGURE CAPTIONS:**

2 Figure 1 (A) Map showing key and speculative areas of terrain during the Palaeogene: BM = Bighorn
3 Mountains; OCM = Owl Creek Mountains; WR = Wind River Ranges; AM = Absaroka Mountains; BTM =
4 Beartooth Mountains; PM = Pryor Mountains; NBL = Nye Bowler Lineament; CA = Cody Arch; WRR =
5 Wind River Ranges; GVR = Grossventre Ranges; TR = Teton Ranges; WIOB = Wyoming Overthrust Belt;
6 TU = Targhee Uplift; BCU = Basin Creek Uplift. Adapted from Love (1973), Seeland (1978), Kraus (1985),
7 Lillegraven (2009) and Finn (2010). (B) Modern extent of the Bighorn Basin with key mountain ranges
8 identified. Locations studied are indicated by location numbers.

9 Figure 2 (A) Graph depicting channel body data for each formation. Note that the average channel body
10 thickness does not vary from the Fort Union Formation into the Willwood Formation, but a slight
11 decrease in channel percentage is noted. (B) Percentage that each channel geometry type (see Table 1
12 for summary of geometries) comprises the Fort Union and Willwood formations channel deposits. Note
13 a change to less amalgamated geometries from the Fort Union Formation into the Willwood Formation.

14 Figure 3 (A) Graphs showing channel body thickness (m) against height in the sedimentary succession
15 (m). The line of best fit and moving averages are recorded on each graph. Data sorted into columns
16 based on correlation strength. (B) Graph showing the cumulative order of CV values. Note that three
17 groups can be observed; low, moderate and high values.

18 Figure 4 (A) Palaeocurrent map, produced from imbricated clast and cross-bedding data from channel
19 deposits. (B) Weighted average grain size (mm) for channel body deposits at each location. (C) Channel
20 percentage at each location. (D) Average channel body thickness (m) for each location. (E) Maximum
21 channel body thickness (m) for each location. (F) Average storey thickness (m) for each location. Large
22 arrows indicate where predicted DFS trends are present (green) and not present (purple).

1 Figure 5 (A) Dominant sandstone geometry (see Table 1 and Owen et al., 2017, for summary of channel
2 body geometries) at each location. (B) Interpreted position on a DFS based on the dominant channel
3 body present at each location. (C) Interpreted position on a DFS based on the channel percentage at
4 each location. (D) Summary diagram showing key source areas/fluvial systems in the basin based on
5 analyses and integration of datasets presented. Coloured block arrows represent the systems defined
6 within this study. Large arrows indicate where predicted DFS trends are present (green) and not present
7 (purple) in (B) and (C).

8 Figure 6: Examples of deposits found at the western margin of the basin. (A) Alluvial fan type facies
9 found in the Beartooth systems, location 1. (B) Perennial amalgamated meander belt deposits from the
10 Absaroka system, location 12. (C) Example of the internal architecture of the Absaroka fluvial system,
11 location 12. (D) Unconformity found in the Washakie fluvial system with dipping Palaeocene (Fort Union
12 deposits) being overlain by flat lying Eocene (Willwood) deposits, location 20 (see Fig. 1 for location
13 numbers).

14 Figure 7: Cross-section across the northern portion of the basin. Note that summary logs are scaled to
15 one-another, but do not represent true thickness of ages. Logs are assigned an approximate position in
16 the stratigraphy based on mammalian age.

17 Figure 8: Cross-section across the southern portion of the basin. Note that summary logs are scaled to
18 one-another, but do not represent true thickness of NALMA zones. Logs are assigned an approximate
19 position in the stratigraphy based on mammalian age.

20 Figure 9: Cross-section across the western margin of the basin. Note that summary logs are scaled to
21 one-another, but do not represent true thickness of NALMA zones. Logs are assigned an approximate
22 position in the stratigraphy based on mammalian age.

1 Figure 10: Cross-section across the centre of the basin. Note that summary logs are scaled to one-
2 another, but do not represent true thickness of ages. Logs are assigned an approximate position in the
3 stratigraphy based on mammalian age.

4 Figure 11: Examples from the axial portion of the basin. (A) Simple ribbon channel deposits within well-
5 developed palaeosol deposits at location 26. (B) Deposits from the axial system in the northern portion
6 of the basin (locations 5 and 6). Note that the deposits here are more amalgamated (geometry IA and
7 OS), with less well-developed palaeosol deposits, compared to that of location 26 (see Fig. 1 for location
8 numbers).

9 Figure 12: Depositional model of the Bighorn Basin during the Palaeogene based on data collected in
10 this study. This model demonstrates the presence of different sized fluvial systems across the basin,
11 with alluvial fan, DFS and an axial system being identified.

12 **TABLE CAPTIONS**

13 Table 1: Summary table of key characteristics for the geometries described within the basin. Taken from
14 Owen et al. (2017b)

15 Table 2: Summary table of key trends within each defined set of systems. See text for detailed
16 discussion.

17

1 **REFERENCE LIST**

2 Allen, P.A., and Allen, J.R.L., 1990, Basin Analysis: Principles and applications: Oxford, UK, Blackwell
3 Scientific Publications, 1-451 p.

4 Assine, M.L., Merino, E.R., Pupim, F. do N., Macedo, H. de A., and Santos, M.G.M. dos, 2015, The
5 Quaternary alluvial systems tract of the Pantanal Basin, Brazil: Brazilian Journal of Geology, v. 45, p.
6 475–489, doi: 10.1590/2317-4889201520150014.

7 Baczynski, A. a., McInerney, F. a., Wing, S.L., Kraus, M.J., Bloch, J.I., Boyer, D.M., Secord, R., Morse, P.E.,
8 and Fricke, H.C., 2013, Chemostratigraphic implications of spatial variation in the Paleocene-
9 Eocene Thermal Maximum carbon isotope excursion, SE Bighorn Basin, Wyoming: Geochemistry,
10 Geophysics, Geosystems, v. 14, p. 4133–4152, doi: 10.1002/ggge.20265.

11 Bown, T.M., and Kraus, M.J., 1983, Ichnofossils of the alluvial Willwood Formation (Lower Eocene),
12 Bighorn Basin, northwest Wyoming, U.S.A.: Palaeogeography, Palaeoclimatology, Palaeoecology, v.
13 43, p. 95–128.

14 Bown, T.M., and Kraus, M.J., 1987, Integration of channel and floodplain suites, developmental
15 sequence and lateral relations of alluvial paleosols: Journal of Sedimentary Petrology, v. 57, p. 587–
16 601, doi: 10.1306/212F8BB6-2B24-11D7-8648000102C1865D.

17 Bown, T.M., and Kraus, M.J., 1981, Lower Eocene alluvial paleosols (Willwood Formation, northwest
18 Wyoming, U.S.A) and their significance for paleoecology, paleoclimatology, and basin analyses:
19 Palaeogeography, Palaeoclimatology, Palaeoecology, v. 34, p. 1–30.

20 Bridge, J.S., 2003, Rivers and floodplains. Forms processes and sedimentary record: Oxford, UK,
21 Blackwell Publishing Ltd.

22 Cain, S.A., and Mountney, N.P., 2011, Downstream changes and associated fluvial-eolian interactions in

1 an ancient terminal fluvial system: The Permian Organ Rock Formation, SE Utah, USA, *in* Davidson,
2 S.K. ed., *From river To rock record: The preservation of Fluvial sediments and their subsequent*
3 *interpretation*, p. 0–19.

4 Catuneanu, O., 2006, *Principles of Sequence Stratigraphy*. Elsevier, Amsterdam

5 Çiftçi, N.B., and Bozkurt, E., 2009, Evolution of the Miocene sedimentary fill of the Gediz Graben, SW
6 Turkey: *Sedimentary Geology*, v. 216, p. 49–79, doi: 10.1016/j.sedgeo.2009.01.004.

7 Clyde, W.C., Hamzi, W., Finarelli, J.A., Wing, S.L., Schankler, D., and Chew, A., 2007, Basin-wide
8 magnetostratigraphic framework for the Bighorn Basin, Wyoming: *Bulletin of the Geological*
9 *Society of America*, v. 119, p. 848–859, doi: 10.1130/B26104.1.

10 Connell, S.D., Kim, W., Paola, C., and Smith, G. a., 2012, Fluvial Morphology and Sediment-Flux Steering
11 of Axial-Transverse Boundaries In An Experimental Basin: *Journal of Sedimentary Research*, v. 82,
12 p. 310–325, doi: 10.2110/jsr.2012.27.

13 Connell, S.D., Kim, W., Smith, G.A., and Paola, C., 2012, Stratigraphic Architecture of An Experimental
14 Basin With Interacting Drainages: *Journal of Sedimentary Research*, v. 82, p. 326–344, doi:
15 10.2110/jsr.2012.28.

16 Davies-Vollum, K.S., and Kraus, M.J., 2001, A relationship between alluvial backswamps and avulsion
17 cycles: an example from the Willwood Formation of the Bighorn Basin, Wyoming: *Sedimentary*
18 *Geology*, v. 140, p. 235–249, doi: 10.1016/S0037-0738(00)00186-X.

19 Davies-vollum, K.S., and Wing, S.L., 1998, Taphonomic, and climatic aspects of Eocene swamp deposits
20 (Willwood Formation, Bighorn Basin , Wyoming): *PALAIOS*, v. 13, p. 28–40.

21 Davidson, S.K., Leleu, S., and North, C.P., 2011, Introduction *in* Davidson, S.K., Leleu, S., andNorth, C.P.
22 *From River to Rock Record: The Preservation of Fluvial Sediments and Their Subsequent*

1 Interpretation, SEPM Special Publication 97, p.1-3.

2 DeCelles, P.G., 2004, Late Jurassic to Eocene evolution of the Cordilleran thrust belt and foreland basin
3 system, western U.S.A.: American Journal of Science, v. 304, p. 105–168.

4 DeCelles, P.G., and Cavazza, W., 1999, A comparison of fluvial megafans in the Cordilleran (Upper
5 Cretaceous) and modern Himalayan foreland basin systems: Bulletin of the Geological Society of
6 America, v. 111, p. 1315–1334, doi: 10.1130/0016-7606(1999)111<1315:ACOFMI>2.3.CO;2.

7 DeCelles, P.G., Gray, M.B., Ridgway, K.D., Cole, R.B., Pivnik, D.A., Pequera, N., and Srivastava, P., 1991,
8 Controls on synorogenic alluvial-fan architecture, Beartooth Conglomerate (Palaeocene), Wyoming
9 and Montana: Sedimentology, v. 38, p. 567–590, doi: 10.1111/j.1365-3091.1991.tb01009.x.

10 Dickinson, W.R., Klute, M.A., Hayes, M.J., Janecke, S.U., Erik, R., Mckittrick, M.A., Olivares, M.D., Klute,
11 M.A., and Hayes, M.J., 1988, Paleogeographic and paleotectonic setting of Laramide sedimentary
12 basins in the central Rocky Mountain region: Geological Society of America Bulletin, v. 100, p.
13 1023–1039, doi: 10.1130/0016-7606(1988)100<1023.

14 Dingle, E.H., Attal, M., and Sinclair, H.D., 2017, Abrasion-set limits on Himalayan gravel flux: Nature, v.
15 544, p. 471–474, doi: 10.1038/nature22039.

16 Fan, M., and Carrapa, B., 2014, Late Cretaceous – early Eocene Laramide uplift, exhumation, and basin
17 subsidence in Wyoming: Crustal responses to flat slab subduction: Tectonics, v. 33, p. 509–529, doi:
18 10.1002/2012TC003221.Received.

19 Finn, B.T.M., 2010, Chapter 6: Subsurface Stratigraphic Cross Sections Showing Correlation of
20 Cretaceous and Lower Tertiary Rocks in the Bighorn Basin , Wyoming and Montana, *in* Petroleum
21 Systems and Geological Assessment of Oil and Gas in the bighorn Basin Province, Wyoming and
22 Montana, p. 1–17.

- 1 Finn, T.M., Kirschbaum, Mark A. Roberts, Stephen B. Condon, S.M., and Roberts, Laura N.R. Johnson,
2 R.C., 2010, Chapter 3: Cretaceous-Tertiary Composite Total Petroleum System (503402), Bighorn
3 Basin, Wyoming and Montana, *in* Petroleum Systems and Geological Assessment of Oil and Gas in
4 the Bighorn Basin Province, Wyoming and Montana: U.S. Geological Survey Digital Data Series
5 DDS-69-V, USGS.
- 6 Foreman, B.Z., 2014, Climate-driven generation of a fluvial sheet sand body at the Paleocene-Eocene
7 boundary in north-west Wyoming (USA): *Basin Research*, v. 26, p. 225–241, doi:
8 10.1111/bre.12027.
- 9 Friend, P.F., and Moody-Stuart, M., 1972, Sedimentation of the Wood Bay Formation (Devonian) of
10 Spitsbergen: Regional analysis of a late orogenic basin: *Norsk Polarinstitut, Nr*, p. 1–77.
- 11 Friend, P.F., Slater, M.J., and Williams, R.C., 1979, Vertical and lateral building of river sandstone bodies,
12 Ebro Basin, Spain: *Journal of the Geological Society*, v. 136, p. 39–46.
- 13 Galloway, W.E., Whiteaker, T.L., and Ganey-Curry, P., 2011, History of Cenozoic North American
14 drainage basin evolution, sediment yield, and accumulation in the Gulf of Mexico basin:
15 *Geosphere*, v. 7, p. 938–973, doi: 10.1130/GES00647.1.
- 16 Gawthorpe, R.L., and Leeder, M.R., 2000, Tectono-sedimentary evolution of active extensional basins:
17 *Basin Research*, v. 12, p. 195–218, doi: 10.1111/j.1365-2117.2000.00121.x.
- 18 Gingerich, P.D., 1983, Paleocene-Eocene faunal zones and a preliminary analysis of Laramide structural
19 deformation in the Clark's Fork Basin, Wyoming, *in* 34th Annual Field conference, Wyoming
20 Geological Association Guidebook, p. 185–195.
- 21 Gingerich, P.D., and Clyde, W.C., 2001, Overview of mammalian biostratigraphy in the Paleocene-Eocene
22 Fort Union and Willwood Formations of the Bighorn and Clarks Fork Basins: University of Michigan

- 1 Papers on Paleontology, v. 33, p. 1–14.
- 2 Hartley, A.J., Weissmann, G.S., Nichols, G.J., and Warwick, G.L., 2010, Large Distributive Fluvial Systems:
3 Characteristics, Distribution, and Controls on Development: Journal of Sedimentary Research, V.80,
4 P.167-183.
- 5 Hartley, A.J., Owen, A., Swan, A., Weissmann, G.S., Holzweber, B.I., Howell, J., Nichols, G., and Scuderi,
6 L., 2015, Recognition and importance of amalgamated sandy meander belts in the continental rock
7 record: Geology, v. 43, p. 679–682, doi: 10.1130/G36743.1.
- 8 Hickey, L.J., 1980, Paleocene stratigraphy and flora of the Clarks Fork Basin: University of Michigan
9 Papers on Paleontology, v. 24, p. 33–49.
- 10 Hickey, L.J., and Yuretich, R., 1997, The Belfry Member of the Fort Union Formation, an allocyclic
11 lacustrine deposit of middle Paleocene age in the Bighorn Basin, Montana and Wyoming, *in*
12 Bighorn Basin: 50 years on the Frontier: Evolution of the geology of the Bighorn Basin:1997
13 Fieldtrip Symposium, p. 38–42.
- 14 Hirst, J.P.P., 1991, Variations in alluvial architecture across the Oligo-Miocene Huesca fluvial system,
15 Ebro Basin, Spain, *in* Miall, A.D. and Tyler, N. eds., The three dimensional facies architecture of
16 terrigenous clastic sediments and its implications for hydrocarbon discovery and recovery, Society
17 of Economic Paleontologists and Mineralogists, p. 111–121.
- 18 Holbrook, J., Scott, R.W., & Oboh-Ikuenobe, F.E., 2006, Base-Level buffers and buttresses: A model for
19 upstream versus downstream control on fluvial geometry and architecture within sequences: Journal of
20 Sedimentary Research, 76, p.162–174.
- 21 Horton, B.K., and Decelles, P.G., 2001, Modern and ancient fluvial megafans in the foreland basin system
22 of the central Andes, southern Bolivia : Implications for drainage network evolution in fold- thrust

1 belts: Basin Research, v. 13, p. 43–63.

2 Van Houten, F.B., 1944, Stratigraphy of the Willwood and Tatman Formations in northwestern
3 Wyoming: Geological Society of America 1987 Annual Meeting and Exposition Program, v. 55, p.
4 165–210, doi: 10.1130/GSAB-55-165.

5 Jones, H.L.L., and Hajek, E. a. A., 2007a, Characterizing avulsion stratigraphy in ancient alluvial deposits:
6 Sedimentary Geology, v. 202, p. 124–137, doi: 10.1016/j.sedgeo.2007.02.003.

7 Jones, H.L., and Hajek, E.A., 2007b, Characterizing avulsion stratigraphy in ancient alluvial deposits:
8 Sedimentary Geology, v. 202, p. 124–137, doi: 10.1016/j.sedgeo.2007.02.003.

9 Kelly, S.B., and Olsen, H., 1993, Terminal fans - a review with reference to Devonian examples:
10 Sedimentary Geology, v. 85, p. 339–374.

11 Kraus, M.J., 1992, Alluvial response to differential subsidence: sedimentological analysis aided by
12 remote sensing, Willwood Formation (Eocene), Bighorn Basin, Wyoming, USA: Sedimentology, v.
13 39, p. 455–470.

14 Kraus, M.J., 1996, Avulsion deposits in Lower Eocene alluvial rocks, Bighorn Basin, Wyoming: Journal of
15 Sedimentary Research, v. 66, p. 354–363.

16 Kraus, M.J., 1985, Early Tertiary quartzite conglomerates of the Bighorn Basin and their significance for
17 paleogeographic reconstruction of northwest Wyoming, *in* Flores, R.M. and Kaplan, S.S. eds.,
18 Cenozoic Paleogeography of West-central United States, Rocky Mountain Section of the Society for
19 SEPM, p. 71–91.

20 Kraus, M.J., 1987, Integration of channel and floodplain suites, II Vertical relations of alluvial paleosols:
21 Journal of Sedimentary Petrology, v. 57, p. 602–612.

1 Kraus, M.J., 2001, Sedimentology and depositional setting of the Willwood Formation in the Bighorn and
2 Clarks Fork Basins, *in* Gingerich, P.D. ed., Paleocene-Eocene Stratigraphy and Biotic change in the
3 Bighorn and Clarks Fork Basins, Wyoming, University of Michigan Papers Paleontology, No 33., p.
4 15–28.

5 Kraus, M.J., and Bown, T.M., 1993, Palaeosols and sandbody prediction in alluvial sequences, *in* North,
6 C.P and Prosser, D.J, eds., Characterisation of Fluvial and Aeolian Reservoirs Geological Society,
7 London, Special Publications, v. 73, p. 23–31, doi: 10.1144/GSL.SP.1993.073.01.03.

8 Kraus, M.J., and Davies-Vollum, K.S., 2004, Mudrock-dominated fills formed in avulsion splay channels:
9 Examples from the Willwood Formation, Wyoming: *Sedimentology*, v. 51, p. 1127–1144, doi:
10 10.1111/j.1365-3091.2004.00664.x.

11 Kraus, M.J., and Gwinn, B., 1997, Facies and facies architecture of Paleogene floodplain deposits,
12 Willwood Formation, Bighorn Basin, Wyoming, USA: *Sedimentary Geology*, v. 114, p. 33–54, doi:
13 10.1016/S0037-0738(97)00083-3.

14 Kraus, M.J., McInerney, F.A., Wing, S.L., Secord, R., Baczynski, A.A., and Bloch, J.I., 2013, Paleohydrologic
15 response to continental warming during the Paleocene–Eocene Thermal Maximum, Bighorn Basin,
16 Wyoming: *Palaeogeography, Palaeoclimatology, Palaeoecology*, v. 370, p. 196–208, doi:
17 10.1016/j.palaeo.2012.12.008.

18 Kraus, M.J., and Middleton, L.T., 1987, Contrasting architecture of two alluvial suites in different
19 structural settings, *in* Ethridge, F.G., Flores, R.M., and Harvey, M.D., eds., Recent developments in
20 fluvial sedimentology contributions from the third international fluvial sedimentology conference.
21 Special publication 39., Tulsa, Oklahoma, Society of Economic Paleontologists and Mineralogists, p.
22 253–262.

- 1 Kraus, M.J., and Wells, T.M., 1999, Recognizing avulsion deposits in the ancient stratigraphical record, *in*
2 Smith, N.D. and Rogers, J. eds., *Fluvial Sedimentology 6*. Special publication of the International
3 Association of Sedimentologists, Oxford, UK, Blackwell Science, p. 251–268.
- 4 Kraus, M.J., Woody, D.T., Smith, J.J., and Dukic, V., 2015, Alluvial response to the Paleocene–Eocene
5 Thermal Maximum climatic event, Polecat Bench, Wyoming (U.S.A.): *Palaeogeography,*
6 *Palaeoclimatology, Palaeoecology*, v. 435, p. 177–192, doi: 10.1016/j.palaeo.2015.06.021.
- 7 Kukulski, R.B., Hubbard, S.M., Moslow, T.F., and Raines, M.K., 2013, Basin-scale stratigraphic
8 architecture of upstream fluvial deposits: Jurassic–Cretaceous Foredeep, Alberta Basin, Canada:
9 *Journal of Sedimentary Research*, v. 83, p. 704–722, doi: 10.2110/jsr.2013.53.
- 10 Lawton, T.F., Schellenbach, W.L., and Nugent, A.E., 2014, Megafan and Axial-River Systems In the
11 Southern Cordilleran Foreland Basin: Drip Tank Member of Straight Cliffs Formation and Adjacent
12 Strata, Southern Utah, USA: *Journal of Sedimentary Research*, v. 84, p. 407–434, doi:
13 10.2110/jsr.2014.33.
- 14 Leeder, M.R., and Gawthorpe, R.L., 1987, Sedimentary models for extensional tilt-block/half-graben
15 basins, *in* Coward, M.P., Dewey, J.F., and P.L. Hancock, *Continental Extensional Tectonics,*
16 *Geological Society, London, Special Publications*, v. 28, p. 139–152, doi:
17 10.1144/GSL.SP.1987.028.01.11.
- 18 Legarreta, L., and Uliana, M.A., 1998, Anatomy of hinterland depositional sequences: Upper Cretaceous
19 fluvial strata, Neuquen Basin, West-Central Argentina, *in* Shanley, K.W. and McCabe, P.J. eds.,
20 *Relative Role of Eustasy, Climate, and Tectonism in Continental Rocks*. SEPM Special Publication No
21 59, Tulsa, Oklahoma, Society of Economic Paleontologists and Mineralogists, p. 83–92.
- 22 Leleu, S., and Hartley, A.J., 2010, Controls on the stratigraphic development of the Triassic Fundy Basin,

- 1 Nova Scotia: implications for the tectonostratigraphic evolution of Triassic Atlantic rift basins:
2 Journal of the Geological Society, v. 167, p. 437–454, doi: 10.1144/0016-76492009-092.
- 3 Lillegraven, J.A., 2009, Where was the western margin of northwestern Wyoming's Bighorn Basin late in
4 the early Eocene? *in* Albright, Ed, Papers on Geology, Vertebrate Paleontology, and Biostratigraphy
5 in Honor of Michael O. Woodburne, Museum of Northern Arizona Bulletin, 65, p. 37–81.
- 6 Love, J.D., 1973, Harebell Formation (Upper Cretaceous) and Pinyon Conglomerate (Uppermost
7 Cretaceous and Paleocene), Northwestern Wyoming: Geological survey Professional Paper 734-A,
8 p. 1–59.
- 9 Mack, G.H., Love, D.W., and Seager, W.R., 1997, Spillover models for axial rivers in regions of continental
10 extension: The Rio Mimbres and Rio Grande in the southern Rio Grande rift, USA: Sedimentology,
11 v. 44, p. 637–652, doi: 10.1046/j.1365-3091.1997.d01-49.x.
- 12 Mack, G.H., and Seager, W.R., 1990, Tectonic control on facies distribution of the Camp Rice and
13 Palomas Formations (Pliocene-Pleistocene) in the southern Rio Grande rift: Bulletin of the
14 Geological Society of America, v. 102, p. 45–53, doi: 10.1130/0016-
15 7606(1990)102<0045:TCOFDO>2.3.CO;2.
- 16 McCarthy, P.J., and Plint, A.G., 1998, Recognition of interfluvial sequence boundaries : Integrating
17 paleopedology and sequence stratigraphy: Geology, v. 26, p. 387–390, doi: 10.1130/0091-
18 7613(1998)026<0387.
- 19 Neasham, J.W., and Vondra, C.F., 1972, Stratigraphy and petrology of the Lower Eocene Willwood
20 Formation, Bighorn Basin, Wyoming: Geological Society of America Bulletin, v. 83, p. 2167–2180,
21 doi: 10.1130/0016-7606(1972)83.
- 22 Nichols, G.J., and Fisher, J.A., 2007, Processes, facies and architecture of fluvial distributary system

1 deposits: *Sedimentary Geology*, v. 195, p. 75–90, doi: 10.1016/j.sedgeo.2006.07.004.

2 Nichols, G.J., and Hirst, J.P.P., 1998, Alluvial fans and fluvial distributary systems, Oligo-Miocene,
3 Northern Spain: Contrasting processes and products: *Journal of Sedimentary Research*, v. 68, p.
4 879–889.

5 Nyberg, B., and Howell, J.A., 2015, Is the present the key to the past? A global characterization of
6 modern sedimentary basins: *Geology*, v. 43, p. 643–646, doi: 10.1130/G36669.1.

7 Owen, A., Ebinghaus, A., Hartley, A.J., Santos, M.G.M., and Weissmann, G.S., 2017, Multi-scale
8 classification of fluvial architecture: An example from the Palaeocene-Eocene Bighorn Basin,
9 Wyoming: *Sedimentology*, doi: 10.1111/sed.12364.

10 Owen, A., Nichols, G.J., Hartley, A.J., and Weissmann, G.S., 2017, Vertical trends within the prograding
11 Salt Wash distributive fluvial system, SW United States: *Basin Research*, v. 29, p. 64–80, doi:
12 10.1111/bre.12165.

13 Owen, A., Nichols, G.J., Hartley, A.J., Weissmann, G.S., and Scuderi, L.A., 2015, Quantification of a
14 distributive fluvial system: The Salt Wash DFS of the Morrison Formation, SW USA: *Journal of*
15 *Sedimentary Research*, v. 85, p. 544–561.

16 Posamentier, H.W. & Allen, G.P., 1999, Siliciclastic sequence stratigraphy - concepts and application -
17 concepts in sedimentology and paleontology 7, *SEPM Society for Sedimentary Geology*, p204.

18

19 Rittersbacher, A., Howell, J.A., and Buckley, S.J., 2014, Analysis Of Fluvial Architecture In the Blackhawk
20 Formation, Wasatch Plateau, Utah, U.S.A., Using Large 3D Photorealistic Models: *Journal of*
21 *Sedimentary Research*, v. 84, p. 72–87, doi: 10.2110/jsr.2014.12.

- 1 Rouse, J.T., 1937, Genesis and structural relationships of the Absaroka volcanic rocks, Wyoming: Bulletin
2 of the Geological Society of America, v. 48, p. 1257–1296.
- 3 Secord, R., Gingerich, P.D., Smith, M.E., Clyde, W.C., Wilf, P., and Singer, B.S., 2006, Geochronology and
4 mammalian biostratigraphy of middle and upper paleocene continental strata, Bighorn Basin,
5 Wyoming: American Journal of Science, v. 306, p. 211–245, doi: 10.2475/04.2006.01.
- 6 Seeland, D., 1998, Late Cretaceous , Paleocene , and Early Eocene Paleogeography of the Bighorn Basin
7 and Northwestern Wyoming, *in* Cretaceous and Lower tertiary Rocks of the Bighorn Basin,
8 Wyoming and Montana; 49th Annual Field Conference Guidebook, p. 1–29.
- 9 Seeland, D., 1978, Sedimentology and Stratigraphy of the Lower Eocene Wind River Formation, Central
10 Wyoming: Thirtieth Annual Field Conference, Wyoming Geological Association Guidebook, p. 181–
11 198.
- 12 Shanley, K., and McCabe, P., 1994, Perspectives on the Sequence Stratigraphy of Continental Strata:
13 AAPG Bulletin, v.78, p.544-568.
- 14 Sinha, R., and Friend, P.F., 1994, River systems and their sediment flux , Indo-Gangetic plains , Northern
15 Bihar , India: Sedimentology, p. 825–845, doi: 10.1111/j.1365-3091.1994.tb01426.x.
- 16 Snyder, W.S., Dickinson, W.R., and Silberman, M.L., 1976, Tectonic implications of space-time patterns
17 of Cenozoic magmatism in the Western United States: Earth and Planetary Science Letters, v. 32, p.
18 91–106.
- 19 Spalletti, L.A., and Colombo, F., 2005, From Alluvial Fan to Playa: An Upper Jurassic Ephemeral Fluvial
20 System, Neuquen Basin, Argentina: Gondwana Research, v. 8, p. 363–383, doi: 10.1016/S1342-
21 937X(05)71141-2.
- 22 Stanistreet, I.G., and McCarthy, T.S., 1993, The Okavango Fan and the classification of subaerial fan

1 systems: *Sedimentary Geology*, v. 85, p. 115–133.

2 Sundell, K.A., 1990, Sedimentation and tectonics of the Absaroka Basin of northwestern Wyoming, *in*
3 Wyoming sedimentation and Tectonics, 41st Annual Field Conference Guidebook, p. 105–122.

4 Walker, R.G., 1984, General Introduction: Facies, Facies Sequences, and Facies Models, *in* Walker, R.G.,
5 Ed., *Facies Models*, Geological Association of Canada, p. 1–9.

6 Walker, R.G., 1990, Perspective Facies Modelling and Sequence Stratigraphy: *Journal of Sedimentary*
7 *Petrology*, v. 60, p. 777–786.

8 Weissmann, G.S., Hartley, A.J., Nichols, G.J., Scuderi, L.A., Olson, M.E., Buehler, H., and Banteah, R.,
9 2010, Fluvial form in modern continental sedimentary basins: Distributive fluvial systems: *Geology*,
10 v. 38, p. 39–42, doi: 10.1130/G30242.1.

11 Weissmann, G.S., Hartley, A.J., Scuderi, L.A., Nichols, G.J., Davidson, S.K., Owen, A., Atchley, S.C.,
12 Bhattacharyya, P., Ghosh, P., Nordt, L.C., Michel, L., and Tabor, N.J., 2013, Prograding distributive
13 fluvial systems - geomorphic models and ancient examples, *in* Dreise, S.G., Nordt, L.C., and
14 McCarthy, P.L. eds., *New Frontiers in Paleopedology and Terrestrial paleoclimatology*. SEPM
15 Special Number 104, p. 131–147, doi: 10.2110/sepmsp.104.16.

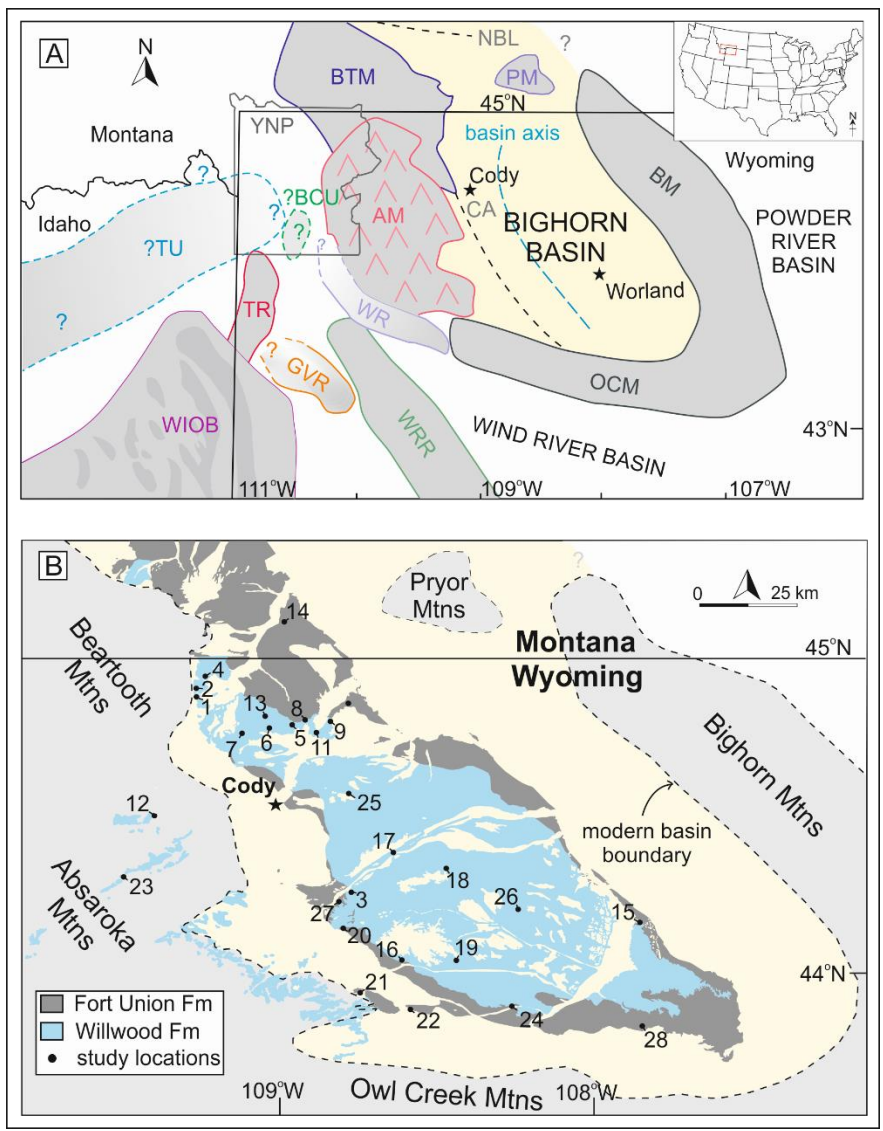
16 Weissmann, G.S., Hartley, A.J., Scuderi, L.A., Nichols, G.J., Owen, A., Wright, S., Felicia, A.L., Holland, F.,
17 and Anaya, F.M.L., 2015, Fluvial geomorphic elements in modern sedimentary basins and their
18 potential preservation in the rock record: A review: *Geomorphology*, v. 250, p. 187–219, doi:
19 10.1016/j.geomorph.2015.09.005.

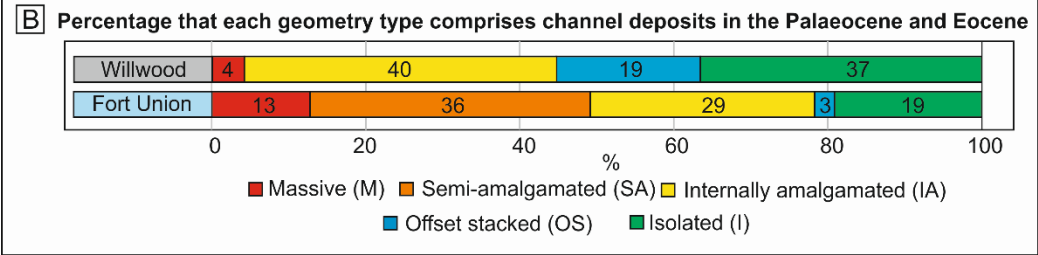
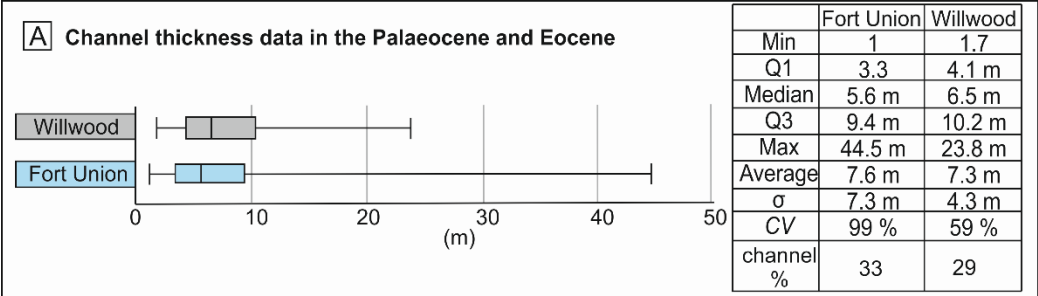
20 Willis, B.J., and Behrensmeier, a. K., 1995, Fluvial systems in the Siwalik Miocene and Wyoming
21 Paleogene: *Palaeogeography, Palaeoclimatology, Palaeoecology*, v. 115, p. 13–35, doi:
22 10.1016/0031-0182(94)00105-H.

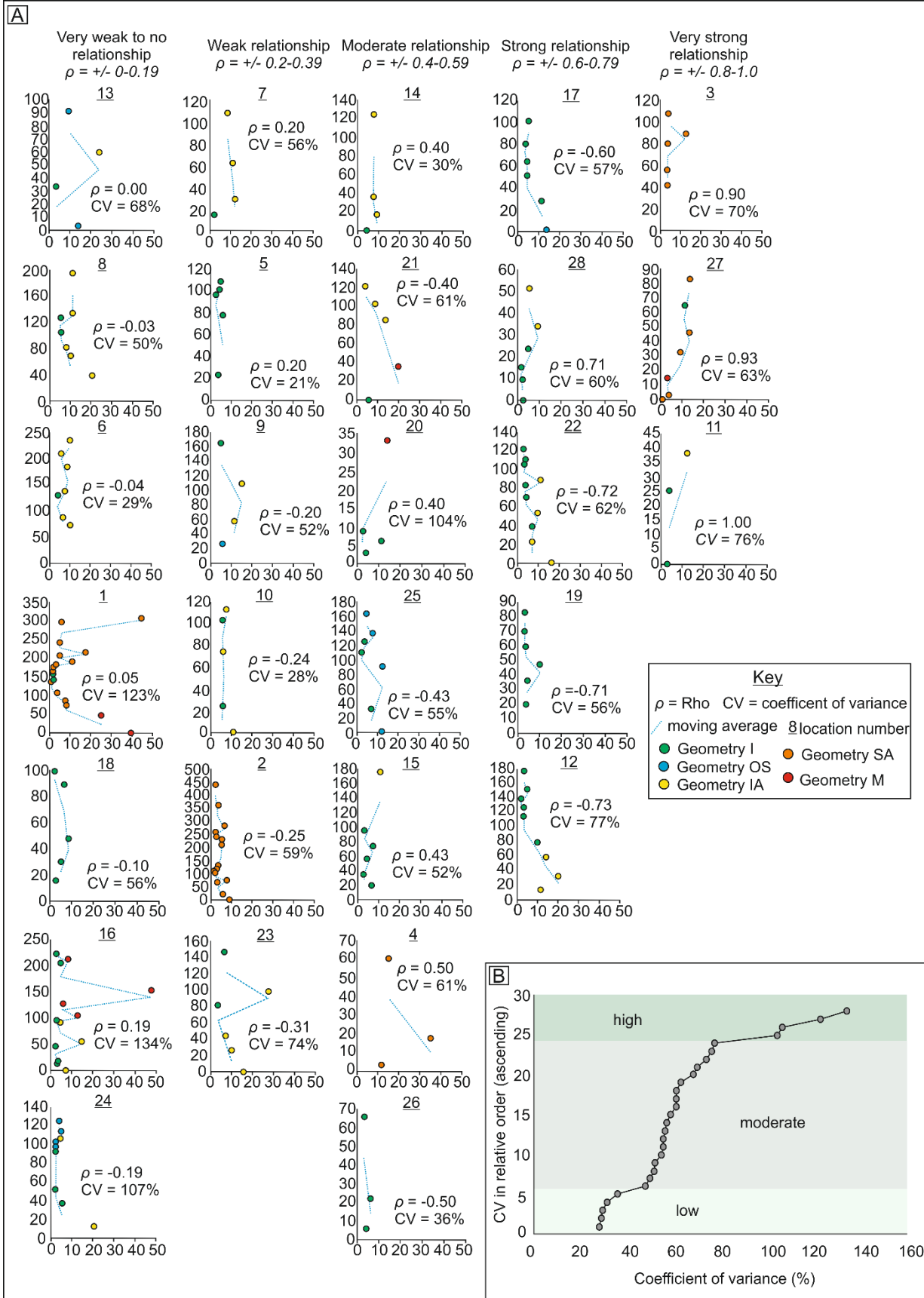
1 Wilson, C.W., 1936, Geology of the Nye-Bowler linement, Stillwater and Carbon Counties, Montana:
 2 Bulletin of the American Association of Petroleum Geologists, v. 20, p. 1161–1188, doi:
 3 10.1126/science.58.1489.27.

4 Yuretich, R.F., Hickey, L.J., Gregson, B.P., and Hsia, Y.L., 1984, Lacustrine deposits in the Paleocene Fort
 5 Union Formation, northern Bighorn Basin, Montana: Journal of Sedimentary Petrology, v. 54, p.
 6 836–852.

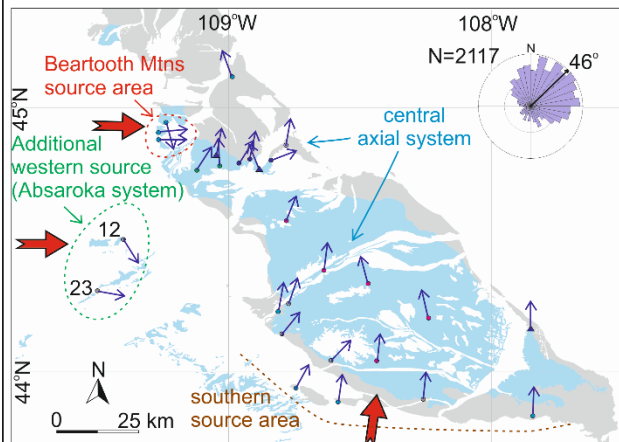
7 **FIGURES**



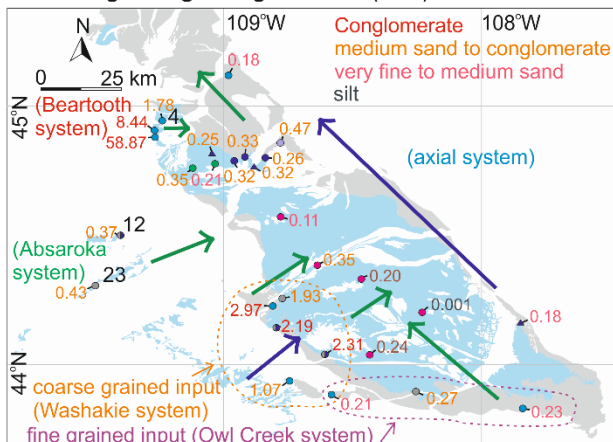




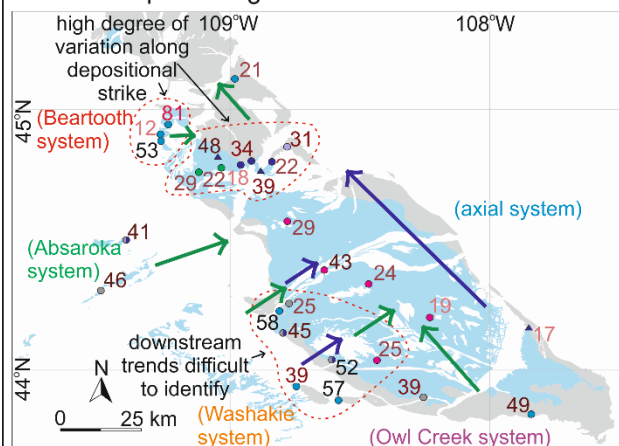
A: Palaeocurrent



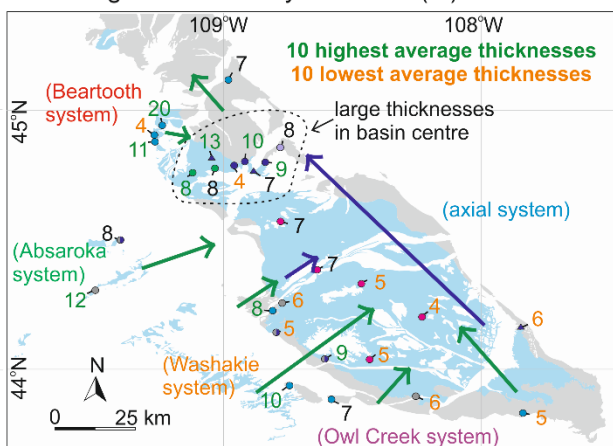
B: Average weighted grain size (mm)



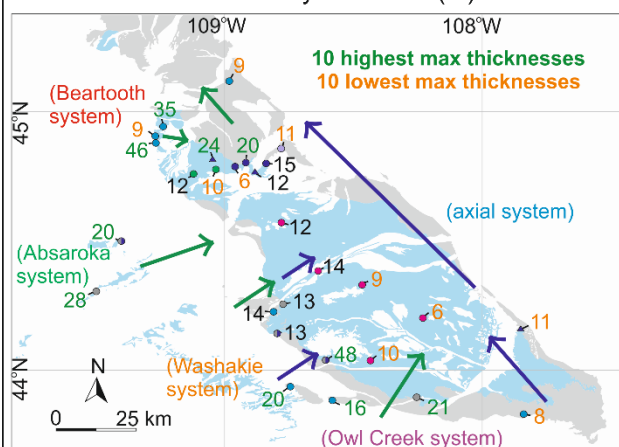
C: Channel percentage



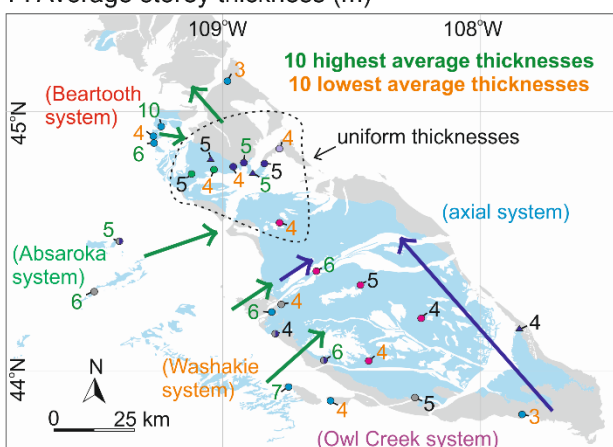
D: Average channel body thickness (m)



E: Maximum channel body thickness (m)



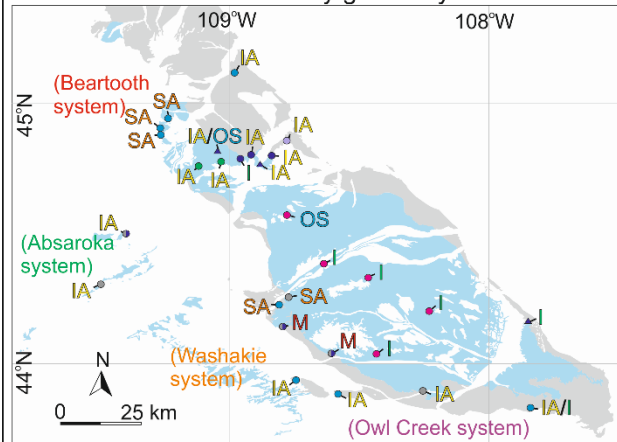
F: Average storey thickness (m)



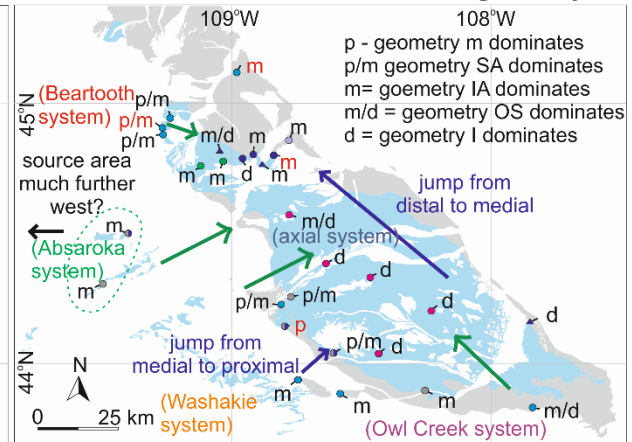
Key

- Paleocene, undiff • Tiffanian • Clarkforkian (+PETM) • Unknown • Unknown/tentative age • Wa-1 through 4 • Wa-5 through 7
- 23 Location number ↗ predicted downstream trends ↖ deviation from predicted downstream trends

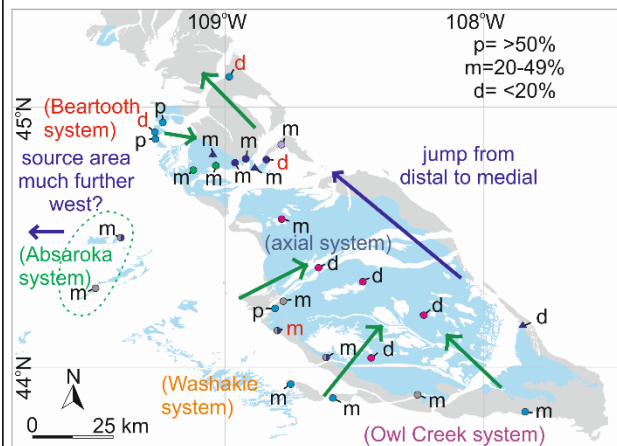
A: Dominant sandstone body geometry



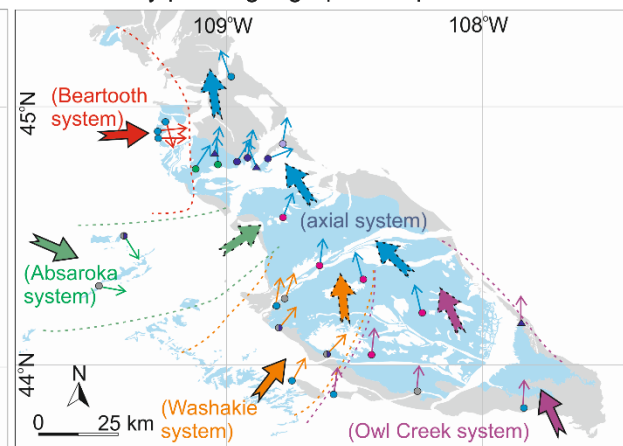
B: Position on a DFS based on channel geometry



C: Position on a DFS based on channel percentage

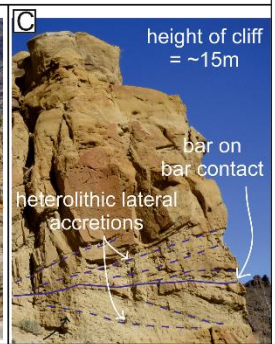
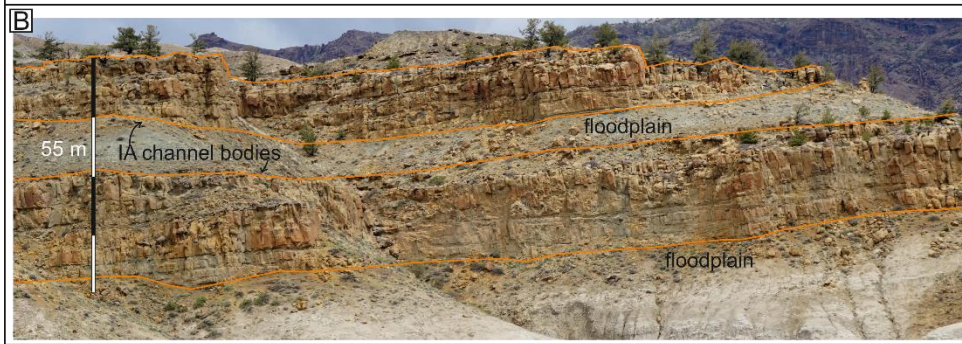
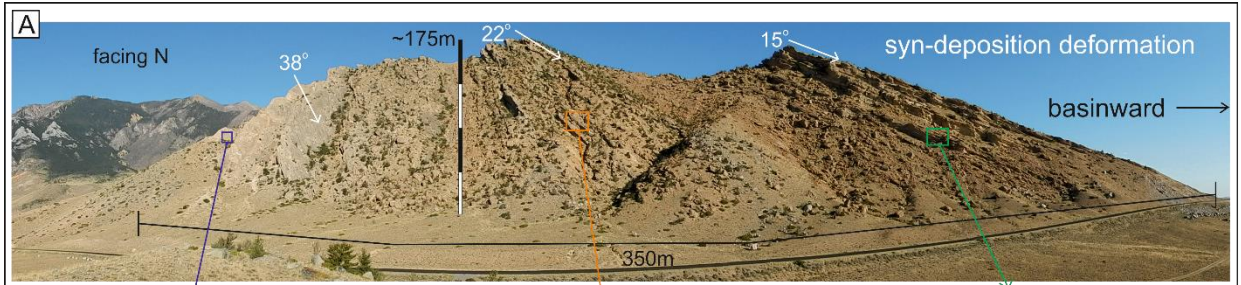


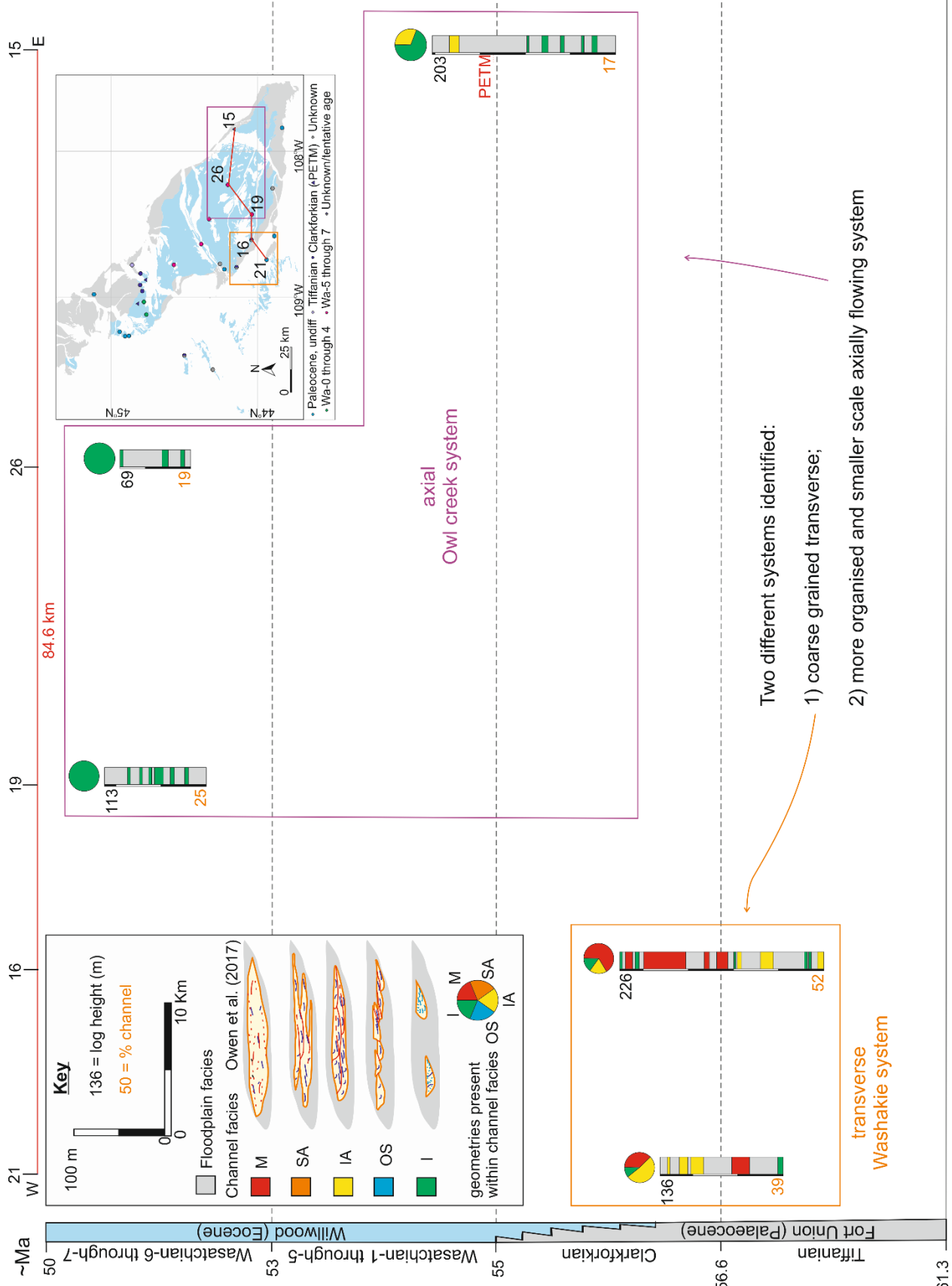
D: Summary palaeogeographic map

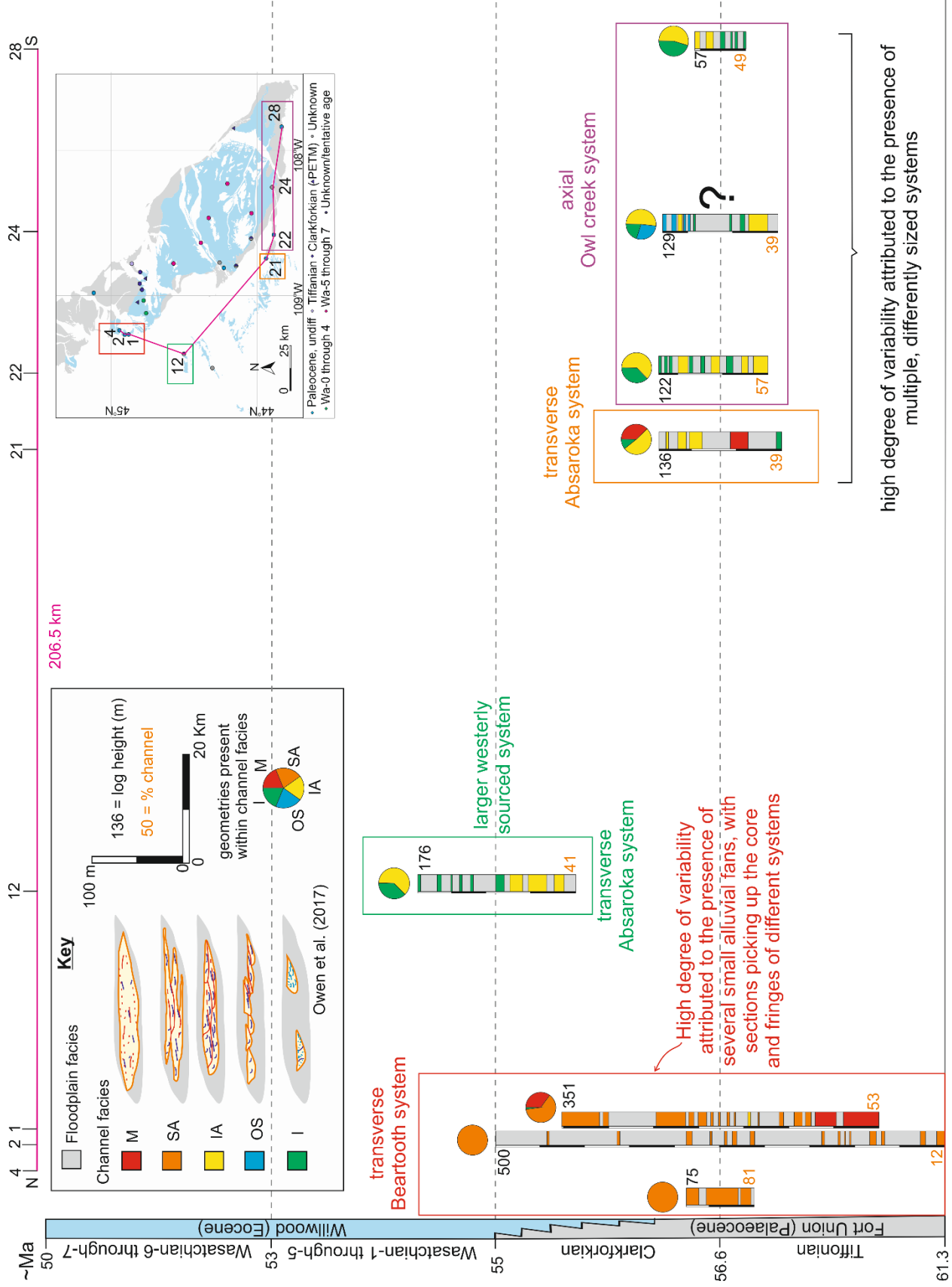


Key

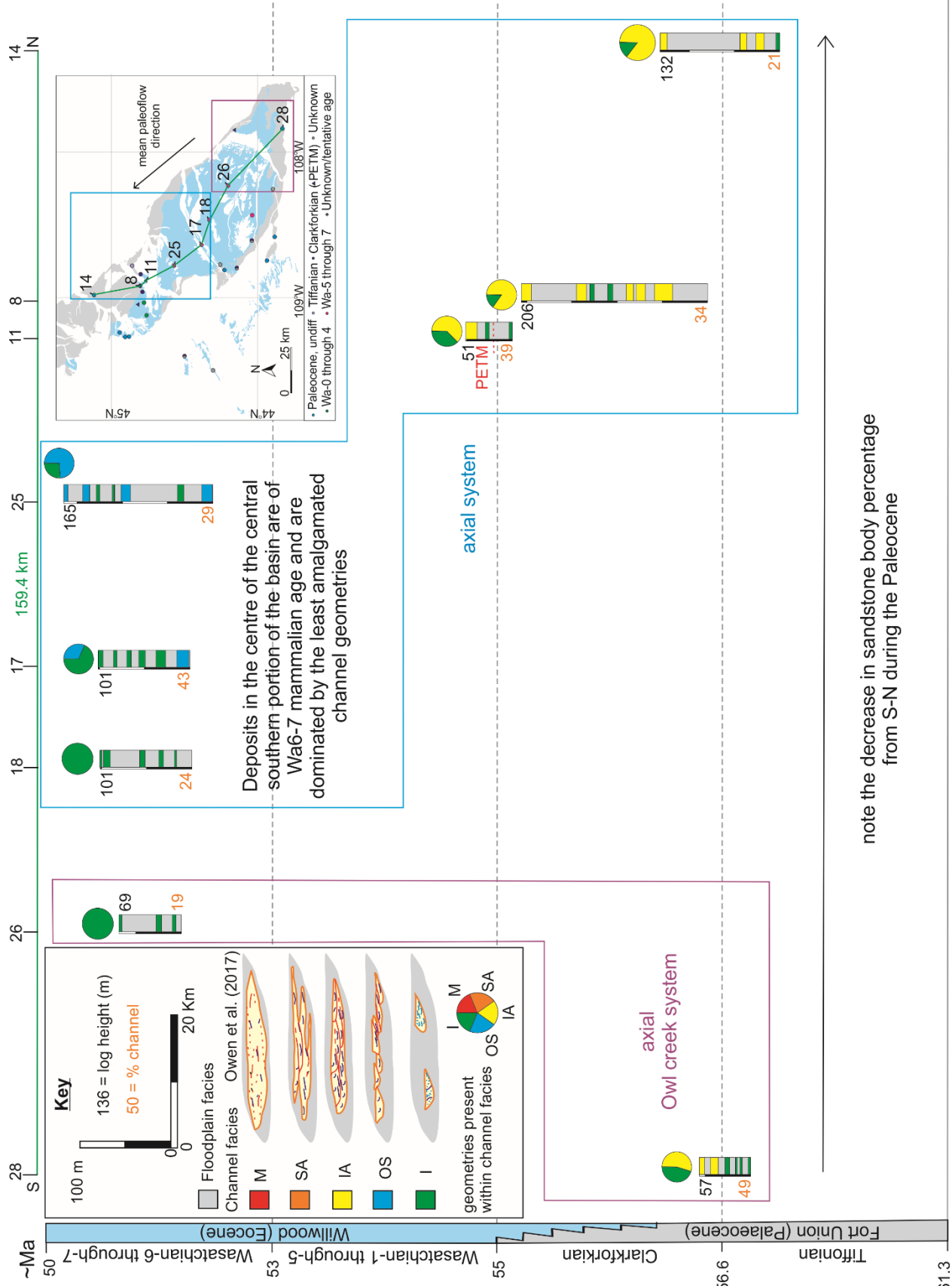
- Paleocene, undiff • Tiffanian • Clarkforkian (•PETM) • Unknown/tentative age • Wa-1 through 4 • Wa-5 through 7
- 23 Location number ↗ predicted downstream trends ↖ deviation from predicted downstream trends

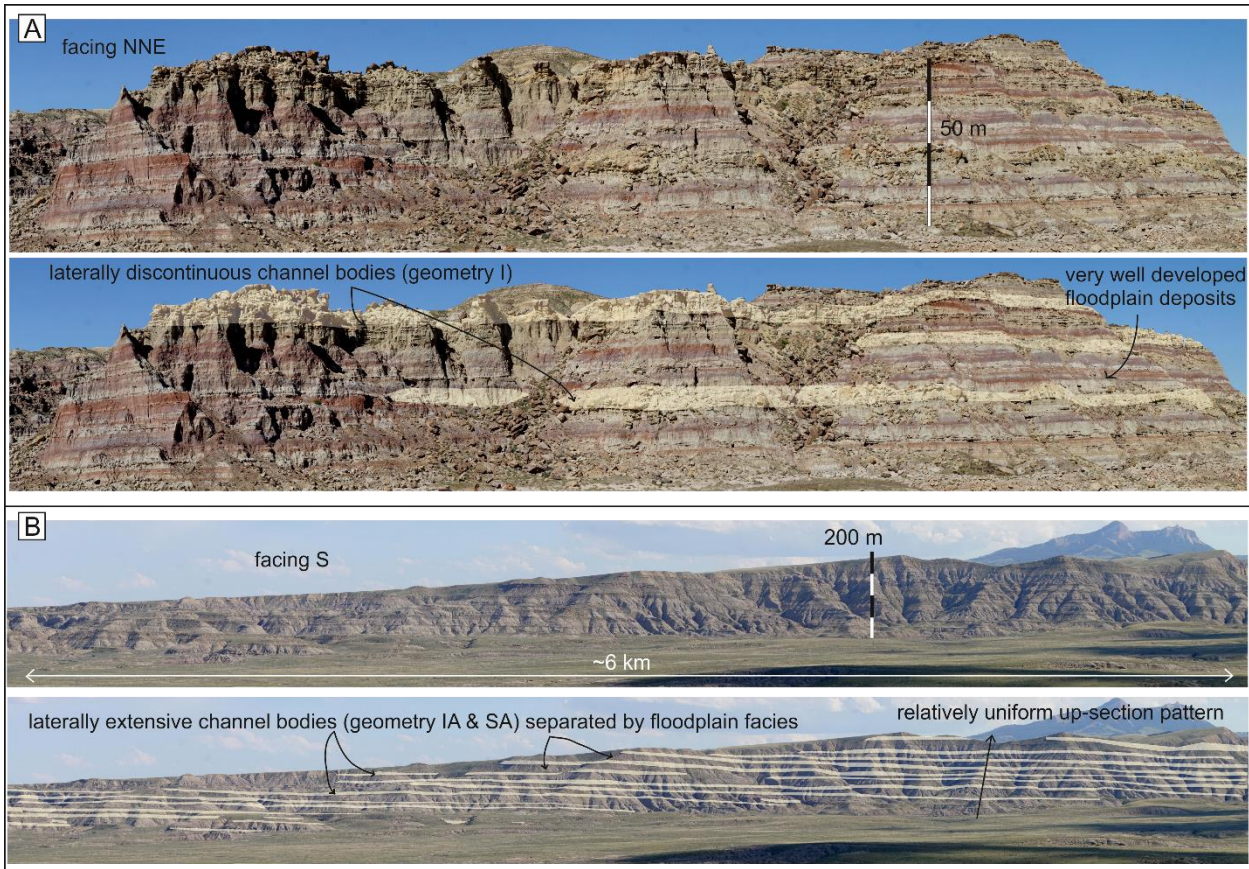




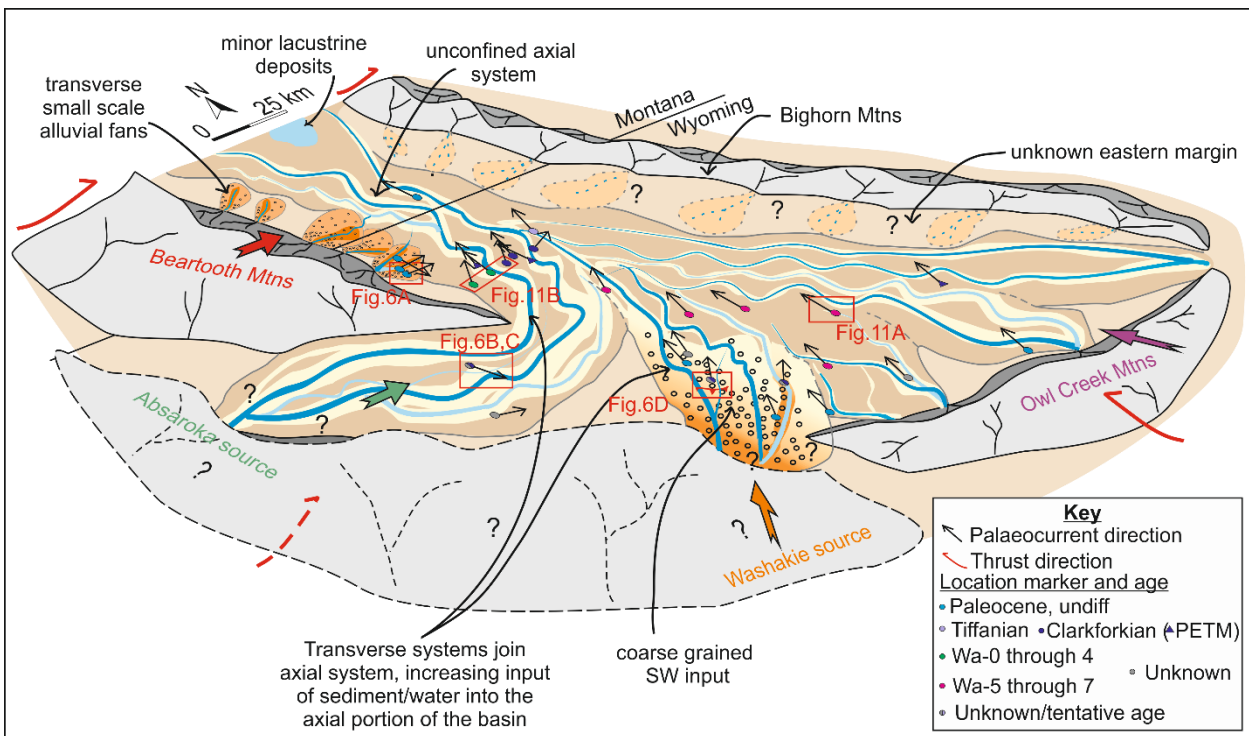


high degree of variability attributed to the presence of multiple, differently sized systems



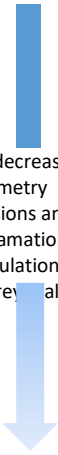
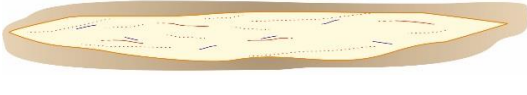
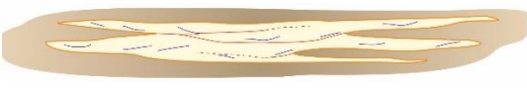





1



2

1 **Tables**

Geometry	Schematic diagram	Description	 <p>General decrease in geometry dimensions and amalgamation (disarticulation at the storey scale)</p>
Massive (M)		Large broad channel geometry Rare storey surfaces that are spatially isolated. Structures difficult to identify.	
Semi-amalgamated (SA)		Broad sheet like bodies are semi-amalgamated with intercalating floodplain deposits. Prevalent storey surfaces.	
Internally Amalgamated (IA)		Broad sheet-like form. Prevalent storey surfaces.	
Offset Stacked (OS)		Storey surfaces are offset stacked resulting in some areas being single storey, and others multistorey. Overall sheet like geometry.	
Isolated (I)		Single storey and disconnected from other channel deposits along strike.	

2

3

	Beartooth	Absaroka	Washakie	Owl Creek	Axial
Grain size	Downstream decrease	Downstream decrease	Variable	Downstream decrease	Downstream increase along much of its length
Channel presence	Downstream decrease	Downstream decrease	Variable	Downstream decrease	Downstream increase along much of its length
Average channel body thickness	Downstream decrease	Downstream decrease	Variable	Downstream decrease	Downstream increase along much of its length
Maximum channel body thickness	Downstream decrease	Downstream decrease	Variable	Variable	Downstream increase along much of its length
Average storey thickness	Downstream decrease	Downstream decrease	Variable	Downstream increase	Variable
Channel geometry	Downstream decrease in amalgamation	Downstream decrease in amalgamation	Variable	Downstream decrease in amalgamation	Downstream increase in amalgamation along much of its length

4

5